Thesis, COLLÉGIALITÉ

Auteur : p236063
Promoteur(s) : 20814
Faculté : Faculté de Médecine
Diplôme : Master en sciences biomédicales, à finalité approfondie
Année académique : 2022-2023
URI/URL : http://hdl.handle.net/2268.2/17838

Université de Liège – Institut de Recherche Labiris

Analysis of a Pseudomonas graminis putative siderophore gene cluster and investigation of the antimicrobial properties of its product on clinical pathogens

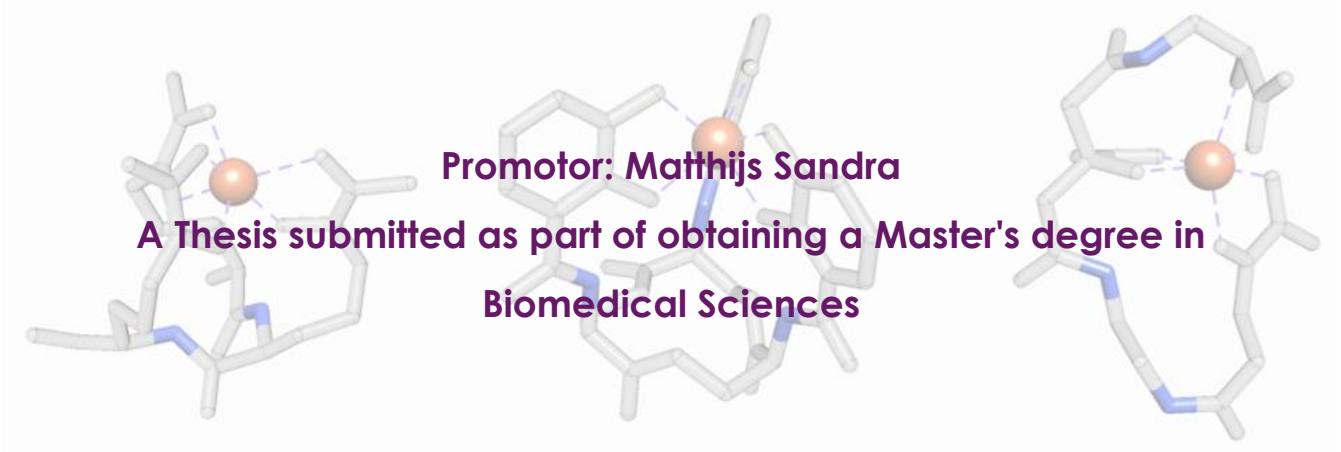

Promotor: Matthijs Sandra

A Thesis submitted as part of obtaining a Master's degree in Biomedical Sciences

Lavender Marie

Academic year 2022-2023 – Master in Biomedical Sciences

Acknowledgments

Primarily, I would like to express my deep appreciation to Alain Durieux for accepting me at Labiris, his research institute, for the completion of my Master's thesis.

Then, I would like to express my heartfelt gratitude to Sandra for initially accepting me into her dedicated research unit, NaturaMonas, and for providing invaluable guidance throughout the writing of my thesis and the commencement of my experiments. Your expertise is truly remarkable, and your unwavering kindness has been a source of comfort during this demanding period. Thank you sincerely for everything you have done.

Other persons from NaturaMonas have also greatly contributed to the completion of this thesis, both practically and theoretically. I would like to express my gratitude to Camille, with whom I had extensive discussions not only about my thesis but also about the world of Research in general. I have learned a lot during these fruitful conversations, and I thank you for being so kind and engaged in my thesis. I would also like to thank Nathalie for supporting me during numerous experiments and for explaining many concepts related to my manipulations. Thanks to the generous donation of clinical strains by Ruben Werquin, I was able to work on a more medical aspect of my topic, and it is with this perspective in mind that I sincerely thank him. It was a true pleasure to work on my thesis in such a learning and enjoyable environment with all of you.

I would like to express my appreciation to my classmates whom I have met during these three years at the University. This Master's program has been filled not only with group projects, collective study sessions at the library, and moments of stress right before exams but also with enjoyable pool parties, spontaneous outings to restaurants, and ski trips. I would like to extend a special thanks to Manon, with whom I share more similarities than one might think. Thank you for being there, even from over 600 km away (Neuchatel-Brussels). Despite the intense moments of pressure, we always managed to motivate each other and bounced back. We're going to earn that diploma, no doubt about it! One last classmate I would like to especially thank is Bahoz. He was my first friend when I arrived at the University, and honestly, I wouldn't have been able to succeed the way I did without him. A big thank you to you, and I'll see you at the graduation ceremony!

Thanks to my family for their beautiful support throughout my studies at the University and Haute École. They have always gone above and beyond to create a comfortable environment for me to study and grow. A special thanks to my mother, who has been the sun in my life, and to Thibault, who has been a true role model.

Thanks to Carine and Pierre for warmly welcoming me during my internship in Brussels and for their kind and caring nature.

Finally, I would like to wholeheartedly thank Victor for being the ultimate source of entertainment and wonderment in my life throughout this past year. I am filled with love and gratitude. Thank you for your boundless patience, comforting presence, unwavering support, and sincere kindness.

Marie

Abstract

Introduction: Given the crisis of multidrug-resistant (MDR) bacteria causing severe infections, the study of siderophores with antimicrobial properties is highly significant. Siderophores, being secondary metabolites notably secreted by bacteria and regulated by iron, exhibit potential for therapeutic use against MDR bacteria. This underscores their potential as promising candidates for combating drug resistance and addressing the challenges associated with MDR infections. This Master's thesis focused on *P. graminis* LMG 21661^T whose genome contains an uncharacterized siderophore gene cluster and studied its potential antimicrobial properties.

Results: *In silico* analysis of the putative gene cluster in *P. graminis* revealed similarities to the gene cluster responsible for the production of marinobactin, a siderophore known to be produced by *Marinobacter* sp. RT-qPCR experiments showed that genes of the siderophore gene cluster were expressed under iron-limiting conditions. A successful purification method isolated the putative siderophore for further LC-MS characterization. LC-MS analyses indicated that marinobactins with shorter acyl chains could be produced by the *P. graminis* strain. LC-MS analysis of strains of the *Pseudomonas lutea* group, to which *P. graminis* belongs, demonstrated that this siderophore is the characteristic one produced within the *P. lutea* group. Importantly, this study represents the first investigation and demonstration of the antimicrobial properties of this particular siderophore. *In vitro* antagonism assays revealed growth-inhibiting effects on various relevant clinical pathogens, including *Staphylococcus capitis*, *Clostridium sporogenes* and *Bacillus cereus*.

Conclusion: In summary, this study sheds light on the production of a putative variant of a known marine siderophore, more adapted to a non-marine lifestyle, in a group of *Pseudomonas* sp., raising questions about their ecological niche and the role of horizontal gene transfer. Furthermore, we have demonstrated the growth-inhibiting properties of the studied siderophore on clinical pathogens, suggesting its potential application in therapy against these strains.

Keywords: siderophores, *Pseudomonas graminis*, antimicrobial properties, alternative therapy to antibiotics.

Résumé

Introduction : Dans un contexte de crise des bactéries multirésistantes causant des infections graves, l'étude des sidérophores dotés de propriétés antimicrobiennes revêt une grande importance. Les sidérophores, en tant que métabolites secondaires sécrétés entre autres par des bactéries et régulés par le fer, présentent un potentiel thérapeutique contre les bactéries multirésistantes. Ce mémoire s'est concentré sur *P. graminis* LMG 21661^T, dont le génome contient un cluster de gènes de sidérophore non caractérisé, et a étudié ses éventuelles propriétés antimicrobiennes.

Résultats : L'analyse *in silico* du cluster de gène putatif chez *P. graminis* a révélé des similarités avec le cluster de gènes responsable de la production de la marinobactine, un sidérophore produit par *Marinobacter* sp. Des expériences de RT-qPCR ont montré que les gènes du cluster de gènes du sidérophore étaient exprimés dans des conditions limitées en fer. Une méthode de purification a permis d'isoler le sidérophore putatif pour une caractérisation ultérieure par LC-MS. Les analyses LC-MS ont indiqué que des marinobactines avec des chaînes acyles plus courtes pourraient être produites par la souche de *P. graminis*. L'analyse LC-MS de souches du groupe *Pseudomonas lutea*, auquel *P. graminis* appartient, a démontré que ce sidérophore est celui caractéristique produit au sein du groupe *P. lutea*. Cette étude représente également la première investigation et démonstration des propriétés antimicrobiennes de ce sidérophore particulier. Des tests d'antagonisme *in vitro* ont révélé des effets inhibiteurs de croissance sur divers pathogènes cliniques pertinents, notamment *Staphylococcus capitis*, *Clostridium sporogenes* et *Bacillus cereus*.

Conclusion : En résumé, cette étude met en lumière la production d'une variante putative d'un sidérophore marin connu, mieux adaptée à un mode de vie non marin, au sein d'un groupe de *Pseudomonas* sp., soulevant des questions sur leur niche écologique et le rôle du transfert horizontal de gènes. De plus, nous avons démontré les propriétés inhibitrices de croissance du sidérophore étudié sur des pathogènes cliniques, suggérant son potentiel d'application en thérapie contre ces souches.

Mots-clés : sidérophores, *Pseudomonas graminis*, propriétés antimicrobiennes, alternative thérapeutique aux antibiotiques.

Abbreviations list

- ABC: ATP-Binding Cassette
- BCCM: Belgian Coordinated Collections of Microorganisms
- CAA: Casamino Acids medium
- CAS: Chrome Azurol S
- dfoB: Deferoxamine or Desferrioxamine B
- FDA: Food and Drug Administration
- Fur: Ferric uptake regulator
- HPLC: High-Performance Liquid Chromatography
- LC-MS: Liquid Chromatography (coupled to) Mass Spectrometry
- LMG: Laboratory of Microbiology – Ghent
- MDR: Multi-Drug Resistant
- MSM: Minimal Succinate Medium
- MQ: water Milli-Q®
- MW: Molecular Weight
- NIS: NRPS-Independent Siderophore
- NMR: Nuclear Magnetic Resonance
- NRPS: Non-Ribosomal Peptide Synthetases
- $OD_{660\ nm}$: Optic Density at 660 nm
- ORFs: Open Reading Frames
- PKS: Polyketide Synthase
- qPCR: Quantitative Polymerase Chain Reaction
- ROS: Reactive Oxygen Species
- Rpm: Revolution Per Minute
- Rt: Retention Time
- SPBP: Siderophore Periplasmic Binding Protein
- TBDT: TonB-dependent transporter

Table des matières

1. Introduction

1.1. *Pseudomonas* genus

1.1.1 *Status of Pseudomonas* taxonomy

Since the description of the genus *Pseudomonas* in 1894, updates of its classification have been done many times and this information is listed in Bergey's Manual. Back in the day (1923), classification was only based on phenotypic characteristics such as Gram-stain, presence of flagellum and oxygen metabolism. When the genetic techniques arrived (1961), the GC content was added in Bergey's Manual to classify the bacteria. In the 1980's, the analysis of the 16S ribosomal RNA gene sequence placed the genus *Pseudomonas* into the Gamma proteobacteria. In the 2000s, a big reclassification of *Pseudomonas* occurred and allowed a new format of the 2015 Bergey's Manual. Since then, the number of bacterial genera and species is continuously increasing and detailed in new versions of Bergey's Manual (Peix et al., 2018).

This dramatic augmentation of new bacterial genera and species is obviously linked to the increase in genome analysis techniques allowing their discovery in diverse types of environments such as soil, water, air, animals, and fungi. This evolution contributes to the enrichment of the knowledge on bacterial biodiversity, specifically in the genus *Pseudomonas* where 70 novel species were described from 2009 to 2018 (Peix et al., 2018).

1.1.2 *Pseudomonas graminis*

Twenty-four years ago, a yellow-pigmented group of bacteria isolated from grasses was studied and characterized as a new species of the *Pseudomonas* genus. It was called *Pseudomonas graminis* since it was isolated from grasses (Behrendt et al., 1999). *P. graminis* belongs to the *P. lutea* group of the *P. fluorescens* lineage. Other *P. graminis* strains have been isolated from the phyllosphere of apples (Mikiciński et al., 2016). A *P. graminis* (PDD-13b-3) was even recovered from cloud water (Besaury et al., 2017). This shows that this bacterium is capable of living in low temperatures and high UV radiation levels.

The type strain of *P. graminis*, *P. graminis* LMG 21661^T, is used in this study since its genome is sequenced, it is a reference strain and it is easy to obtain. The strain is characterized by the production of a yellow pigment (Figure 1). *P. graminis* does not produce a fluorescent pigment contrary to many *Pseudomonas* spp. such as *P. aeruginosa* and *P. fluorescens*. It has a single polar flagellum, and the ability to produce siderophore (Behrendt et al., 1999).

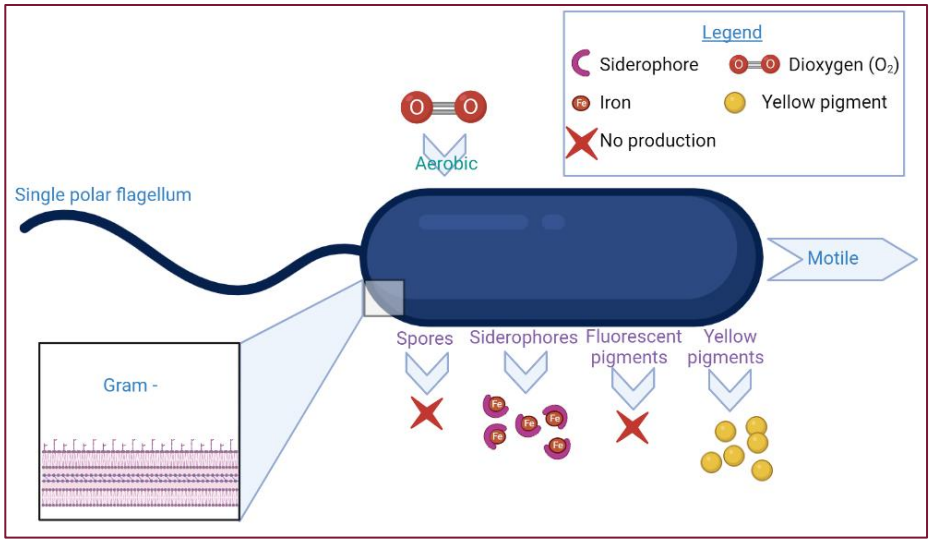

Figure 1: Schematic representation of *Pseudomonas graminis* LMG 21661^T and a few of its structural and biochemical features based on the description by Behrendt et al., 1999. Image created with Biorender.

1.2. Bacterial siderophores

1.2.1 Functions and structure

Iron is an essential element for all living entities on earth. Since it acts as an efficient redox catalyst (Carroll and Moore, 2018), it is necessary for diverse cellular processes such as oxidative phosphorylation, biosynthesis of aromatic compounds and amino acids, and the electron transfer chain. Due to iron's low bioavailability, bacteria (as well as fungi) have developed siderophores which give them the ability to survive in iron-limiting conditions (Khasheii et al., 2021).

The word "siderophore" comes from a Greek word meaning "iron bearer" (Saha et al., 2013). Siderophores are small molecules with a molecular weight ranging from 300 to 2000 Da, exhibiting a strong affinity for ferric iron (Khasheii et al., 2021). Each siderophore possesses a specific affinity for iron, and different conventions are employed to represent this affinity. The most widely used convention is the pM(etal) or pFe value, which is determined based on a standard concentration of free iron (1 µM) and the siderophore (10 µM) at a pH of 7.4 (Butler et al., 2021). Siderophores are secreted outer the cell in case of iron starvation in parallel with the expression of receptors of siderophore-iron complexes (Carroll and Moore, 2018). A bacteria can produce more than one siderophore, *e.g. Klebsiella pneumoniae* produces four siderophores including enterobactin, yersiniabactin, salmochelin, and aerobactin in order to improve tissues colonization and/or avoid neutralization by host proteins in case of human infections (Paczosa and Mecsas, 2016).

The structure of these siderophores can be very variable. Pyoverdine is the characteristic siderophore produced by fluorescent pseudomonads and contains a chromophore responsible for its fluorescence (Saha et al., 2013). The chromophore is attached to a peptide chain of 6-14 residues. Currently more than 100 structurally different pyoverdines have been described (Hider and Kong, 2010).

The natural biodiversity of siderophores and the important number of these molecules gave rise to their classification in four major families (Figure 2). Since most siderophores use negatively charged oxygen atoms to bind ferric iron, their classification is based on the moiety that donates oxygen: catecholate, hydroxymate, carboxylate and mixed-types (Khasheii et al., 2021).

- Hydroxamate siderophores are mostly found in fungi and filamentous Gram-positive bacteria such as *Streptomyces*. Each hydroxamate group involves two oxygen atoms in a link with ferric iron. Desferrioxamine B (dfoB) is a siderophore produced by *Streptomyces pilosus* containing 3 hydroxamates (Khasheii et al., 2021).
- Catecholate siderophores are only produced by bacteria. Each catecholate group also gives two oxygen atoms to form a hexadentate octahedral complex in order to chelate ferric iron (Khasheii et al., 2021). Enterobactin is an example of catecholate siderophore that contains 3 catecholates and is produced by Gram-negative bacteria, such as *Escherichia coli*, *Salmonella typhimurium* and *Klebsiella pneumoniae* (Wilson et al., 2016).
- Carboxylate siderophores are both produced by bacteria and fungi. Rhizobactin is secreted notably by *Rhizobium meliloti* and contains an ethylenediamine D-carboxylic acid and hydroxycarboxyl structure responsible for iron chelation (Khasheii et al., 2021). Staphyloferrin A, produced by *Staphylococcus hyicus,* contains 4 carboxylate moieties for binding Fe^{3+} (Wilson et al., 2016).
- Mixed-type siderophores are divided into four groups: catecholate hydroxymate, phenolate hydroxymate, citrate catecholate and citrate hydroxymate. Pyoverdine is able to bind iron with three moieties: two hydroxamates and one catecholate (Wilson et al., 2016). Yersiniabactin, produced notably by *Yersinia pestis* and *Klebsiella pneumoniae*, includes phenolate, thiazole, oxazoline and carboxylate groups to bind iron (Khasheii et al., 2021).

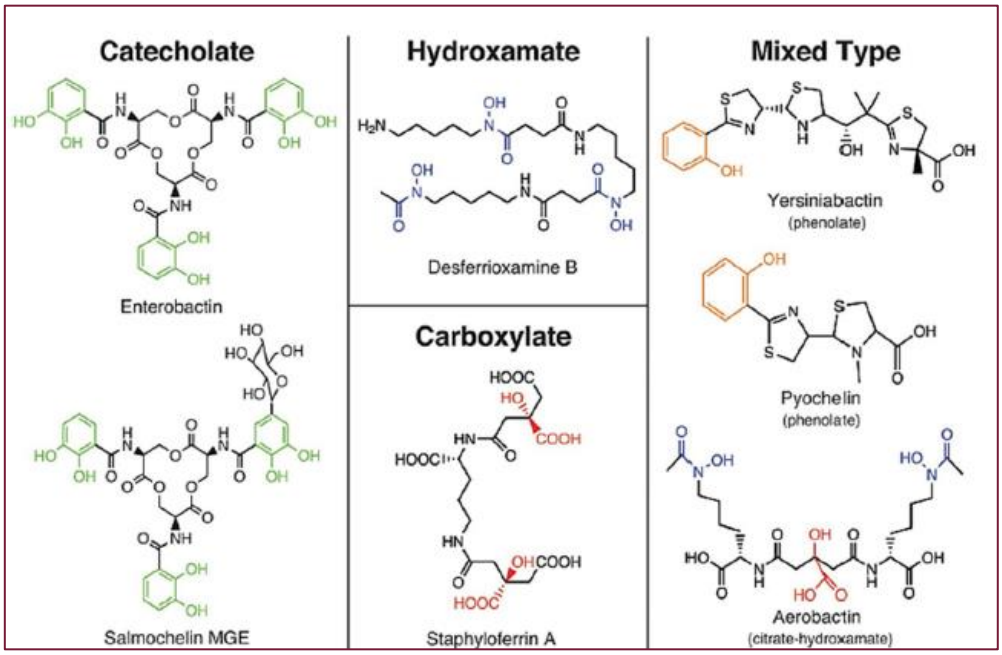

Figure 2: Representation of the four classes of siderophores based on the chemical group involved in iron binding (Khasheii et al., 2021).

1.2.2 Biosynthesis and uptake of siderophores

1.2.2.1 Biosynthesis

Biosynthesis of siderophores is accomplished through a variety of enzymes: non-ribosomal peptide synthetases (NRPS), polyketide synthases (PKS), and/or NRPS-independent siderophore (NIS) synthetases (Carroll and Moore, 2018; Lamb, 2015).

NRPS biosynthesis

Proteins are synthesized employing ribosomes. Siderophores as well as antibiotics (*e.g.* penicillin and vancomycin) use another pathway for their biosynthesis: enzymes called Non-Ribosomal Peptide Synthetases (NRPS) (Mootz et al., 2002).

Peptides from NRPS pathway are small (1 to 48 amino acids long) but more than 300 different substrates can be used to build the peptide (proteinogenic and "unnatural" residues containing for example D-configurated amino acids, N-methylated amino acids, and hydroxy acids). This high diversity contrasts with the ribosomal machinery which uses only 20 amino acids (Konz and Marahiel, 1999). Further modifications such as adenylation, acylation, glycosylation or heterocyclization can increase diversity of NRPS peptides (Mootz et al., 2002).

NRPSs are large enzymes that function in an assembly line mode. These enzymes are modular, which means that they are all organized following the same pattern of modules: a unique initiation module, (multiple) elongation module(s) and a unique termination module. Each module is composed of several domains (Figure 3). This variety of domains gives NRPS a certain specificity on which amino acid is added. This particularity of domains specificity is used to predict peptide structure based on NRPS gene (refer to section *3.2. In silico analyses*) (Mootz et al., 2002).

These domains represent a particular function incorporated/ modified in the peptide. Four domains are named major, because they are present in all the modules: Adenylation domain (A), Peptide Carrier Protein domain (PCP), Condensation domain (C) and Termination domain (TE). Six domains are accessory: Formylation domain (F), Methylation domain (M), Cyclisation domain (Cy), Oxidation domain (Ox), Reduction domain (R) and Epimerization domain (E).

- The **Adenylation domain** allows the recognition of a specific amino acid and adenylates it by using ATP (Figure 3A).
- The **Peptide Carrier Protein** (PCP) domain is consistently located downstream of the Adenylation domain. The PCP domain facilitates the attachment of the activated amino acid to a thioester, which is bound to the ppan (4'-phosphopantetheinyl) factor. The PCP domain itself is connected to ppan through a 4'-phosphopantetheinyl transferase. Unlike other domains, the PCP domain does not possess catalytic activity, as the thiolation process is catalyzed by the Adenylation domain. The initiation module typically consists of an Adenylation domain and a PCP domain (Figure 3B).

- The **Condensation domain** allows the formation of a peptide bound between the amino acid/peptide linked to the initiation module and the amino acid linked to the elongation module (Figure 3C).
- The **Termination domain** is exclusively found in the termination module and serves the purpose of releasing the newly formed peptide. Once released, the peptide undergoes either cyclization or hydrolysis, providing clues about its structural configuration (cyclic if cyclization and linear if hydrolysis) (Figure 3D).
- **Accessory domains** can increase peptide diversity by modifying it *via* various reactions. Formylation domain which is found in the initiation module can tailor the peptide chain by the addition of a formylated residue (Reimer et al., 2019). An epimerization domain enables the incorporation of D-configurated amino acids thanks to the epimerization of L-configurated amino acids. A methylation domain enables the incorporation of N-methylated amino acids. A cyclization domain enables a peptide backbone to be cyclized. A reduction domain enables to reduce heterocycles by adding two electrons. This phenomenon is present in the biosynthesis of the siderophores yersiniabactin and pyochelin (Sieber and Marahiel, 2005). Oxydation domain catalyzes the oxidation of molecules incorporated in the peptide under construction. Colibactin is an example of bacterial toxin produced by *E. coli* and other *Enterobacteriaceae* whose bioactivity is due to the oxidation of thiazoline in thiazole (Pang et al., 2020).

Some of these modifications (such as epimerization) protect the peptide from proteolytic digestion.

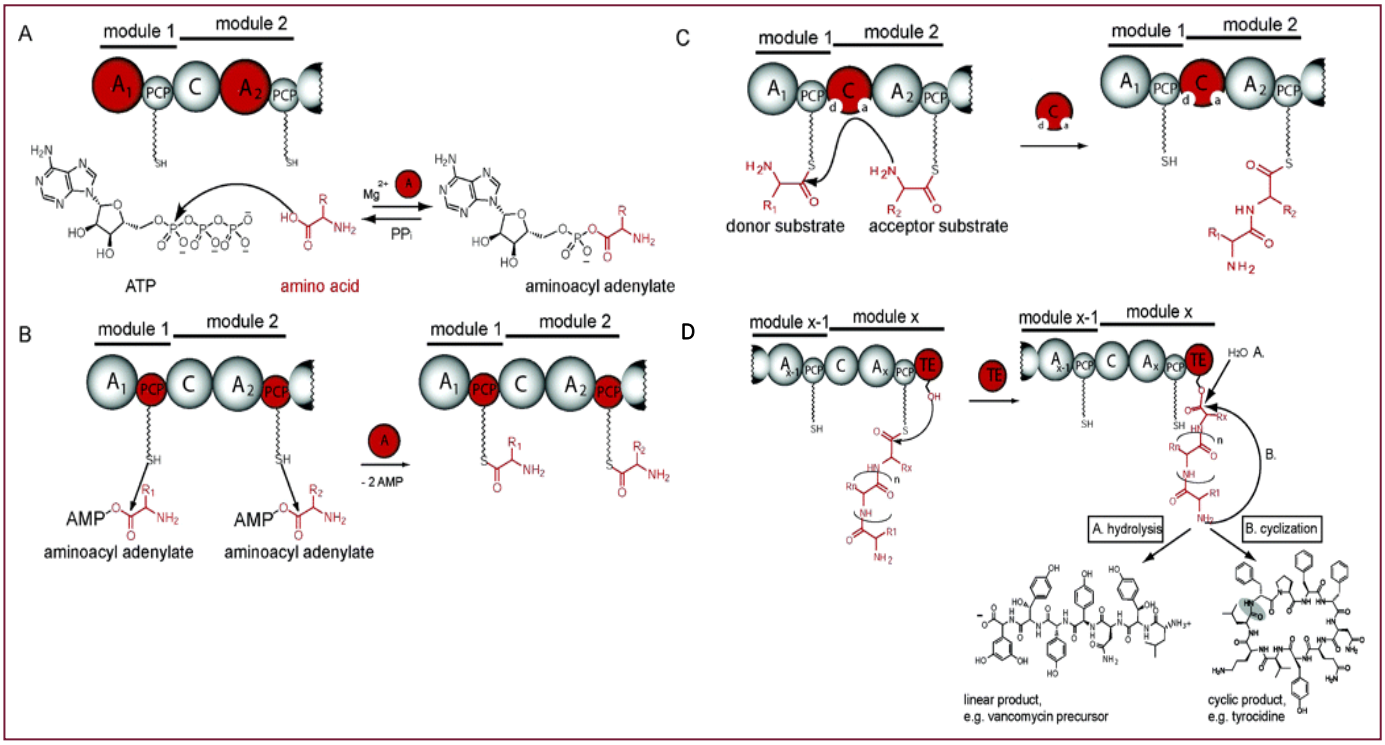

Figure 3: Schematic representation of peptide synthesis by the NRPS pathway. Domains in each module of NRPS enzymes are represented as well as their role in peptide synthesis. Modified from Sieber and Marahiel, 2005.

PKS biosynthesis

PKSs are multifunctional enzymes implied in biosynthesis of polyketide natural products (Quadri, 2014) such as rapamycin and lovastatin (Lim et al., 2016). Siderophores can be constructed by PKS enzymes if their biosynthesis requires the insertion of other functionalities into the backbone (Lamb, 2015) because they are structurally and functionally analogous to fatty acid synthases (Fujii et al., 2001). There are 3 classes of PKS based on their number of subunits and mode of synthesis: type I which is divided into iterative type I and assembly-line type I, type II and type III (Nivina et al., 2019).

There are six different catalytic domains (Figure 4) in PKS:

- The three minimum required for each PKS are β-Ketosynthase (KS), Acyl Transferase (AT), and Acyl Carrier Protein (ACP). The AT domain is responsible for loading the starter, extender, and intermediate acyl units onto the PKS assembly line. The ACP domain serves as a platform to hold the growing polyketide chain as a thiol ester (KS-S-polyketide). The KS domain facilitates the condensation reaction between the starter, intermediate, and extender units (Lamb, 2015).
- Ketoreductase (KR), Dehydratase (DH), and Enoyl Reductase (ER) domains are additional ones (Sabatini et al., 2018). The KR domain catalyzes the reduction of β-ketone groups to hydroxyl groups. The DH domain reduces hydroxyl groups to enoyl groups (unsaturated). Lastly, the ER domain reduces enoyl groups to alkyl groups (saturated) (Lamb, 2015).

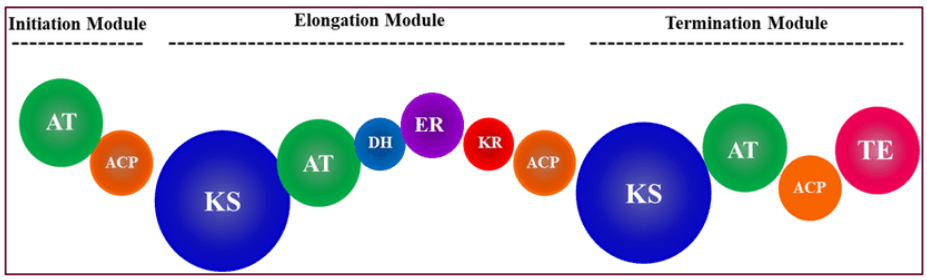

Figure 4: Schematic representation of the PKS modules. The elongation module in a typical PKS is composed of the KS (ketosynthase), AT (acyltransferase), and ACP (acyl-carrier) domains and accessory domains such as DH (dehydration), ER (enoylreductase), and KR (ketoreductase). Modified from Moreira et al., 2020.

NIS synthetase biosynthesis

These enzymes are present in all domains including fungi, archaea and bacteria and are members of the adenylating superfamily. In contrast with NRPS enzymes, NIS enzymes are not modular and do not contain domains (Butler et al., 2021). Their role is to condense a carboxylic acid with an amine or an alcohol to form a peptide or an ester bond using a molecule of ATP. Based on their specificity to different carboxylic acids and their known functions NIS enzymes are classified in four subtypes: A, A', B and C (Hoffmann et al., 2020). They function primarily in the biosynthesis of polycarboxylate or mixed-type siderophores (Carroll and Moore, 2018). DesD is an example of type C NIS enzyme in *Streptomyces coelicolor* responsible for the biosynthesis of the desferrioxamines such as dfoB (Figure 5).

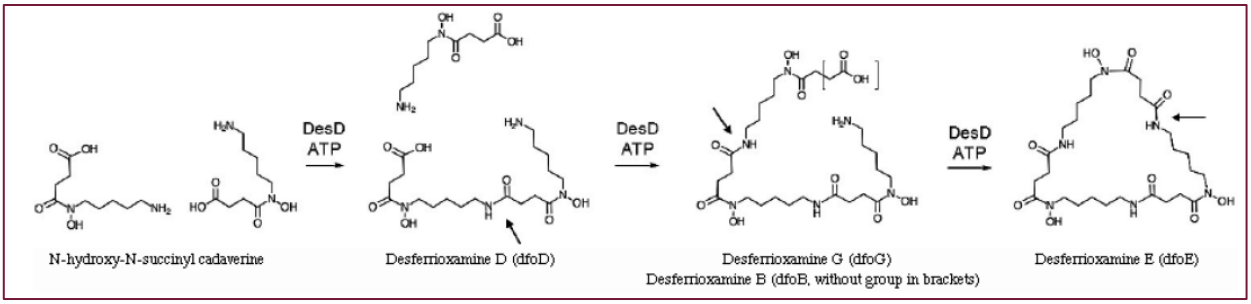

Figure 5: Biosynthesis of desferrioxamines (D, G, B, and E) by DesD. Each peptide bond links diamine and dicarboxylic acids using a molecule of ATP. Each desferrioxamine is an intermediate of the iterative biosynthesis by DesD (Hoffmann et al., 2020).

Another example of NIS siderophore is the recently predicted siderophore triabactin (Grosse et al., 2023).

1.2.2.2 Transport and regulation

In general, siderophore biosynthesis takes place within the cell to be secreted outside the cell in iron-limiting conditions. The secreted siderophore chelates iron in the extracellular medium and becomes a ferric siderophore (Carroll and Moore, 2018).

In **Gram-negative bacteria** (Figure 5), the uptake of ferric siderophores involves a TonB-dependent transporter (TBDT). This TBDT recognizes and transports the ferric siderophore across the outer membrane into the periplasmic space. The energy required for this process is derived from the protonmotive force across the inner membrane. The passage of the ferric siderophore through the inner membrane is facilitated by a siderophore periplasmic binding protein (SPBP), which works in concert with TonB. The SPBP binds to the ferric siderophore and facilitates its transfer to an ATP-Binding Cassette (ABC) transporter located in the inner membrane. The ABC transporter utilizes ATP hydrolysis to power the translocation of the ferric siderophore across the inner membrane into the cytoplasm of the cell. Once in the cytoplasm, iron is reduced by an iron reductase to be released from the siderophore. The siderophore is then reused or degraded. Iron is further used in biological processes. High levels of extracellular iron repress transcription of iron transport genes by binding to the Fur (Ferric uptake regulator) protein. Under iron starvation, iron does not bind Fur which is no longer able to bind the Fur box and the corresponding genes can be transcribed (Carroll and Moore, 2018; Noinaj et al., 2010).

In **Gram-positive bacteria**, there is a single membrane, so the TBDT, SPBP and TonB complex are not present (Carroll and Moore, 2018).

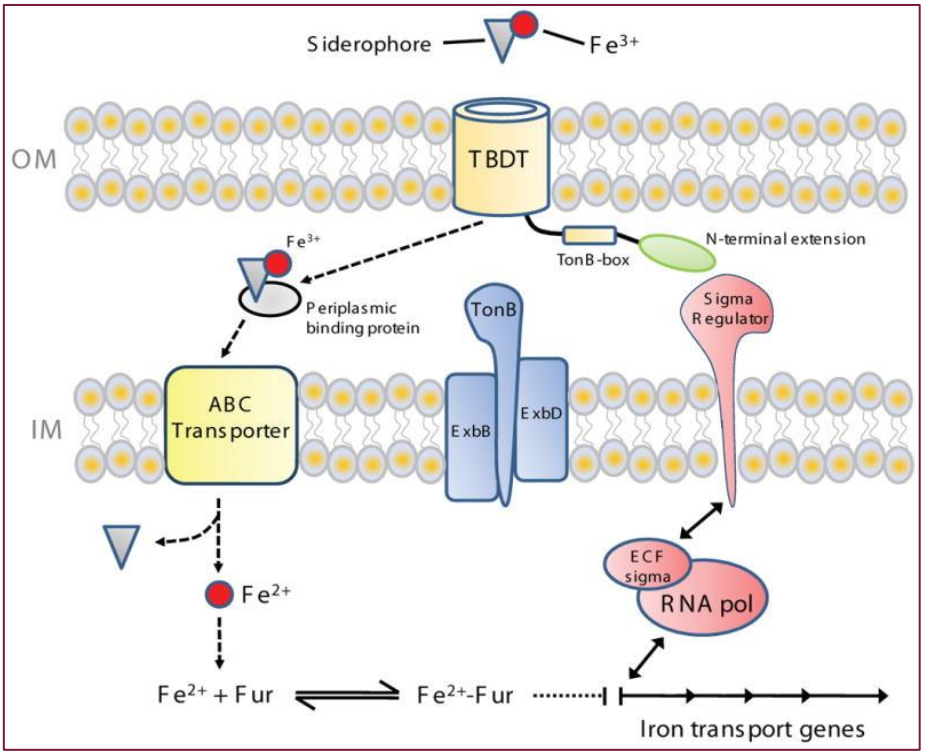

Figure 5: Schematic representation of general siderophore transport and regulation in Gram-negative bacteria (Noinaj et al., 2010).

Some exceptions exist concerning this transport process. Mycobactin, a siderophore primarily produced by the *Mycobacterium* genus, differs from extracellular siderophores such as carboxymycobactins and exochelins in that it is not secreted. Instead, it functions as an intracellular siderophore. One hypothesis to explain the presence of this intracellular siderophore is that *Mycobacterium* species have a thick and lipophilic cell envelope, which necessitates a "short-term iron storage system before iron can be transported into the cytoplasm". The intracellular localization of mycobactin allows for efficient iron acquisition and utilization within the unique cellular environment of *Mycobacterium* (Ratledge and Dover, 2000). Some marine bacteria have also been shown to produce extremely lipophilic siderophores unable to diffuse into the extracellular medium. These siderophores would then form little vesicles (Galvis et al., 2020; Martinez et al., 2003).

Iron is the major key regulating siderophore biosynthesis although other extrinsic parameters can also play a role such as pH, temperature and other metals (zinc, cobalt, aluminum *etc*.) (Wilson et al., 2016). As an example, pyoverdine and pyochelin, notably produced by *P. aeruginosa*, can also bind Ag^{+}, Al^{3+}, Cd^{2+}, Co^{2+}, Cr^{2+}, Cu^{2+}, Eu^{3+}, Ga^{3+}, Hg^{2+}, Mn^{2+}, Ni^{2+}, Pb^{2+}, Sn^{2+}, Tb^{3+}, Tl^{+} and Zn^{2+} but less efficiently (Saha et al., 2013). Siderophore production can also be regulated by oxygen as has been shown for a *Pseudomonas stutzeri* strain. Indeed, under aerobic growth conditions *P. stutzeri* was able to produce four different siderophores (ferrioxamines E, G, D2 and X1) while under anaerobic growth conditions none of them were produced (Essén et al., 2007). As well as biosynthesis and production, transport systems are specific for each siderophore.

1.2.3 Ecological consequences of siderophore secretion at the community level

The siderophore system represents a highly effective strategy to combat iron deficiency; however, it introduces important considerations regarding bacterial communities.

One fundamental concept is that siderophores might not always find their way back to their producing cell when bacteria are in planktonic form contrary to biofilm form. This loss due to diffusion can be dramatic and even compromise fitness of the bacteria (Kramer et al., 2019). Some bacteria have therefore developed strategies to overcome this problem, through the addition of a lipopeptide tail to the siderophore to anchor it to the membrane or *via* the formation of vesicles. This phenomenon is encountered in marinobactins, siderophores produced by the *Marinobacter* sp. strain DS40M6 (Martinez et al., 2003).

A first consequence of siderophore diffusion is **cooperation**. This defines the fact that secreted siderophores can be shared between cells to accelerate iron uptake thanks to a common siderophore. The advantage of cooperation is an important fitness saving (Kramer et al., 2019).

The second consequence of siderophore diffusion arises from the unstable evolution of cooperation and is known as **cheating**. This phenomenon occurs among closely related cells. Certain selfish cells can stop siderophore production but keep the matching receptor as an exploitation of producing cells to save energy and resources. Producing cells can limit the cheaters by mechanisms based on cell density, spatial structure and regulatory circuits (Kramer et al., 2019).

The notion of cheating does not only evolve from the one of cooperation. Cheaters can be cells that were never siderophore producers, indeed receptors can be acquired by horizontal gene transfer (Wilson et al., 2016).

Pseudomonas aeruginosa is an opportunistic pathogen that, in addition to its own siderophore receptors for pyoverdine and pyochelin, contains multiple receptors for xenosiderophores (xeno- : stranger) (Chan and Burrows, 2023) (Figure 6). As has been shown in a study on a siderophore-negative mutant, *Streptomyces coelicolor* can utilize the siderophore from a neighbouring fungus (Arias et al., 2015). This notion not only exists in bacteria but also in yeasts, *Saccharomyces cerevisiae* does not produce siderophores but has siderophore-iron uptake systems to utilize siderophores produced by other microorganisms (Wilson et al., 2016).

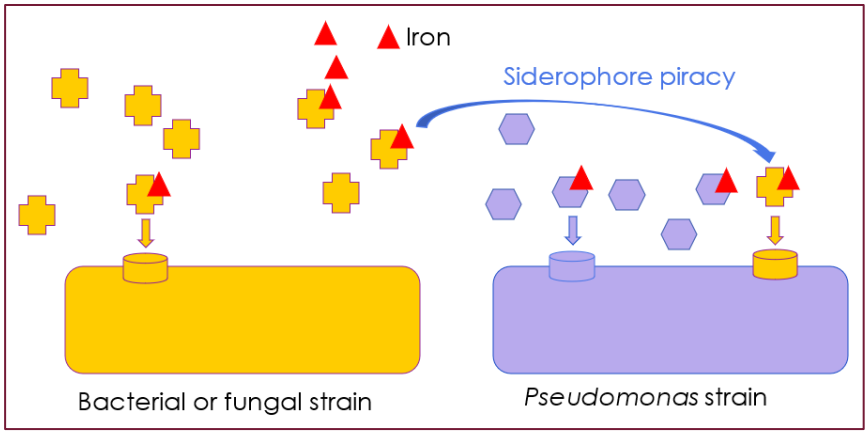

Figure 6: Schematic representation of siderophore piracy between a *Pseudomonas* strain (cheater cell) and another bacterial or fungal strain. The *Pseudomonas* strain is able to take up iron from a xenosiderophore (yellow) thanks to a matching receptor (yellow) without producing this siderophore. Production of another siderophore (purple) from the cheater cell, can be present or not.

A third consequence of siderophore diffusion is **competition**, which involves interactions between non-closely related cells, in contrast to cooperation and cheating. During competition, siderophores function as competitive molecules in an iron-restricted environment, where iron is sequestered and reserved by a specific siderophore for uptake by the producing bacteria. Bacteria lacking matching receptors for the specific siderophore are at a disadvantage because the iron from the medium is partially or completely captured and no longer available to them. If two siderophore-producing bacteria without matching receptors for each other's siderophores coexist in an iron-restricted medium, the amount and pM value (affinity) of secreted siderophores, as well as the flexibility of siderophore production, become critical factors for survival (Kramer et al., 2019).

So, siderophores are important key factors in viability of producing cells but also of non-producing cells. These concepts are not exclusive to bacteria but are relevant to all living organisms that require and produce siderophores.

1.2.4 Involvement of siderophores in bacterial infections in humans

Obtaining iron is a common challenge for bacterial communities and even more difficult in the presence of human iron-binding proteins such as heme and transferrin present in body fluids (Carroll and Moore, 2018). The bacterial uptake of iron can be harder when siderophores are directly blocked by human proteins called siderocalin (Sia et al., 2013).

Bacteria have therefore developed strategies to circumvent these challenges, *e.g.*, acidification of the medium, secretion of enzymes such as ferric oxidoreductase/permeases and hemolysins (Carroll and Moore, 2018), direct uptake of iron from host proteins (Ratledge and Dover, 2000) and production of "stealth" siderophores able to escape human "innate" immune system. Petrobactin is an example of "stealth" siderophore produced notably by *Bacillus anthrasis* and not recognized by siderocalin (Oves-Costales et al., 2007).

Moreover, this battle becomes a real arms race due to the appearance of more human proteins whose role is to block siderophores. Lactoferrin is released by white blood cells around an infection and binds to two iron ions to insure a low level of iron. Tear lipocalin (lipocalin 2 or Lcn2) directly binds to siderophores and more particularly catecholate-type ones (Correnti and Strong, 2012; Golonka et al., 2019).

The "Iron Tug-of-War" continues when bacteria produce some evolved siderophores and/or competitive antagonists able to bind to human proteins. *Klebsiella pneumoniae* can release a "stealth" siderophore called 2,3-dihydroxybenzoylserine (DHBS) that binds to Lcn2 (Golonka et al., 2019). As mentioned earlier, *Klebsiella pneumoniae* can also produce more than one siderophore to escape the human "innate" immune system (Figure 7). Indeed, enterobactin which is the primary produced siderophore, can be inhibited by Lcn2. Structural changes in enterobactin occur to give an evolved siderophore, salmochelin, that can no longer be inhibited by Lnc2 and is a c-glucosylated form of enterobactin. Yersiniabactin and aerobactin are two other siderophores not recognized by Lnc2 (Paczosa and Mecsas, 2016).

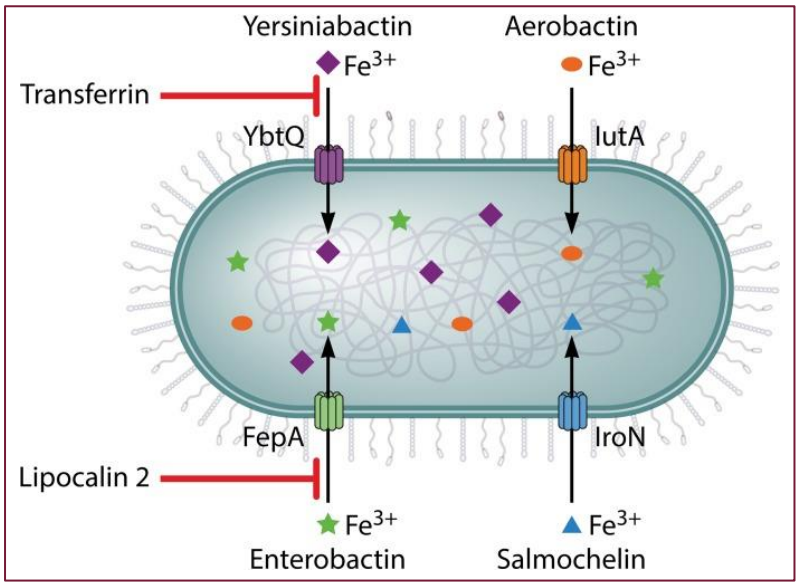

Figure 7: Schematic representation of *Klebsiella pneumoniae*, a Gram-negative bacterium able to produce four different siderophores (Paczosa and Mecsas, 2016).

Siderophores play a critical role in bacterial survival both within and outside the host, making them attractive targets for combating infections in humans. As an alternative or combination therapy of antibiotics, siderophores can also be exploited to directly tackle infections in humans (Page, 2019).

1.2.5 Medical exploitations of siderophores

1.2.5.1 Treatment for infections caused by MDR bacteria

Using siderophores as "Trojan horses"

With the increase in antibiotic resistance in bacteria, siderophores were envisioned as "Trojan horses" (Figure 8). "Trojan horses" can deliver drugs directly inside the MDR bacteria when conjugated with antibiotics or other therapeutic agents. The principle exploits the siderophore secretion/reuptake system to overcome acquired resistance mechanisms by avoiding passing through porin channels (Wilson et al., 2016).

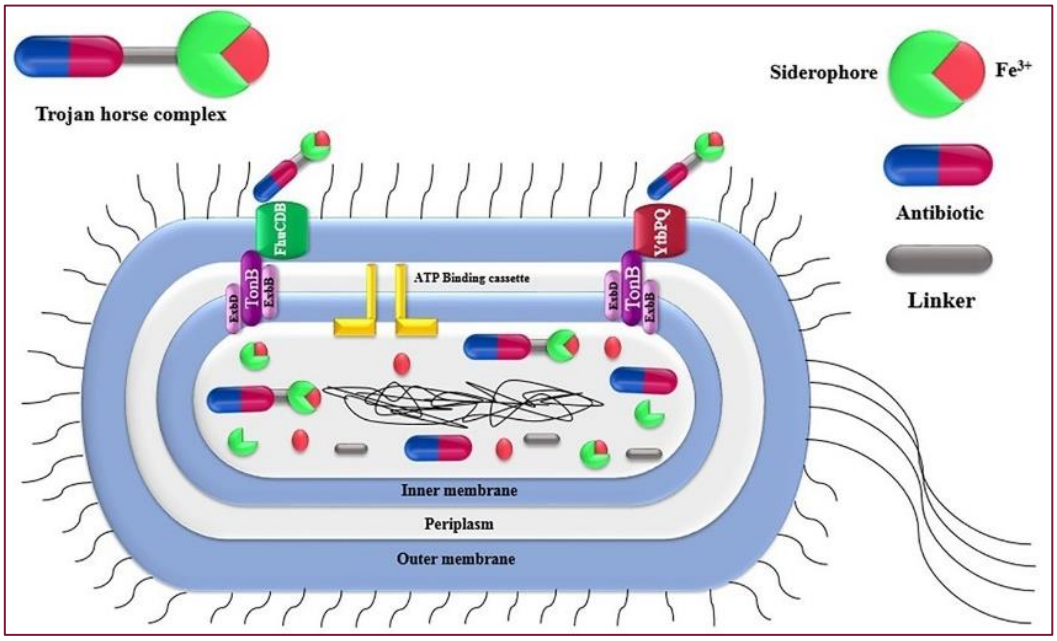

Figure 8: "Trojan horse" strategy using siderophores conjugated to drugs. This complex enters the cell *via* siderophore receptors, then is hydrolyzed to release the drug intracellularly in order to deploy its effects in the cell (Khasheii et al., 2021).

This new advance in therapy for MDR bacterial infections is called sideromycins. They are a group of antibiotics linked covalently to siderophores. They can be natural such as albomycin and salmycin, semi-synthetic such as rifamycin derivative CGP 4832 (derived from the siderophore rifamycin) or synthetic such as Cefiderocol (Braun et al., 2009). Cefiderocol has been approved by the FDA (Food and Drug Administration) in 2019 and is therefore the first siderophore-drug conjugate in the market. It is a siderophore synthetically conjugated with β-lactam antibiotics (Figure 9). This drug targets Gram-negative bacteria, including strains with carbapenem resistance such as *Acinetobacter baumannii*, *Pseudomonas aeruginosa* and *Stenotrophomonas maltophilia*. Cefiderocol is used in urinary tract infections caused by MDR bacteria (Al Shaer et al., 2020; Ito et al., 2016).

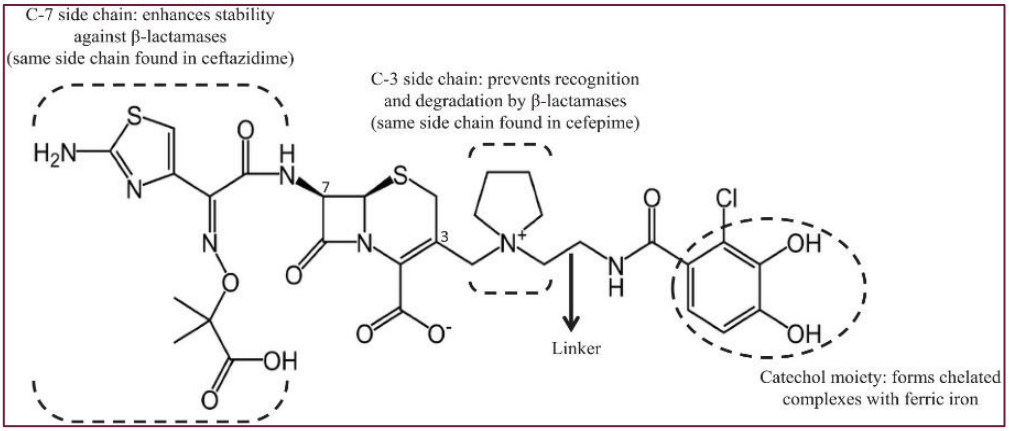

Figure 9: The chemical structure of Cefiderocol and the different parts responsible for the antimicrobial properties (El-Lababidi and Rizk, 2020).

Another example is from a study in 2011 (Miller et al., 2011). It has been reported that a complex comprising the siderophore mycobactin conjugated to artemisinin, an antimalarial agent, exhibited efficacy against MDR strains of *M. tuberculosis* while retaining its antimalarial activity. This innovative approach combines the iron uptake mechanism of mycobactin with the antimicrobial properties of artemisinin, resulting in a dual action against both drug-resistant tuberculosis and malaria.

Using approaches to circumvent siderophores activity

Enhanced understanding of the biosynthesis and mode of action of siderophores has paved the way for the development of therapeutic alternatives by targeting newly discovered molecules.

Firstly, gallium compounds such as Ga^{3+}-maltolate are now used as potential therapeutic agents against methicillin resistant *Staphylococcus aureus* (MRSA). Indeed, Ga^{3+} can compete with ferric iron by binding to all siderophores but cannot participate in biological processes necessary for the maintaining of the cell (Wilson et al., 2016). This strategy showed great results against planktonic cells as well as biofilms of *P. aeruginosa* by reducing growth and biofilm formation (Saha et al., 2013).

Secondly, it is also possible to pharmacologically target the siderophore biosynthesis, secretion or import pathways with specific enzymes inhibitors (Wilson et al., 2016). For example, the MbtA inhibitor salicyl-AMS (5'-O-(N-salicylsulfamoyl)) has been shown to inhibit 2,3-dihydroxybenzoate-AMP ligase (MbtA), an important enzyme in mycobactin biosynthesis leading to suppression of *M. tuberculosis* in infected lungs of mice (Lun et al., 2013). The non-recognition of NIS siderophores by siderocalin confers some pathogens a dramatic virulence (Hoffmann et al., 2020). NIS inhibitors have therefore been investigated to get rid of staphyloferrin B produced by *Staphylococcus aureus* and petrobactin produced by *Bacillus anthracis* that highly contribute to the virulence of these strains. The novel antibiotics baulamycins A and B were isolated from *Streptomyces tempisquensis* and displayed an *in vitro* activity against SbnE and AsbA, respectively NIS of staphyloferrin B and petrobactin (Tripathi et al., 2014).

Thirdly, siderophores have been shown to be closely related to quorum sensing as they cooperatively regulate the biological processes in bacteria such as virulence factors and biofilm formation. Moreover, some microbial resistance mechanisms are known to be regulated by quorum sensing systems. Based on this joint activity, the discovery of siderophores inhibitors could inhibit quorum sensing as well as biofilm formation to tackle chronic infections induced by quorum sensing and caused by MDR bacteria (Yin et al., 2022).

The use of siderophores in therapy raises a crucial question regarding their potential to bind all available iron in the body. The key factor here is the affinity of siderophores for iron compared to that of human iron-binding proteins. If the siderophores have lower affinity for iron than these proteins, they are theoretically unlikely to sequester iron from essential physiological processes and would therefore be considered safe for therapeutic use in humans. However, further research is necessary to fully explore and understand this aspect.

1.2.5.2 Treatment for cancer cells

One thing that surely distinguishes cancer cells from normal cells is their increased demand for nutrients to support continuous and extensive proliferation. Iron is among the essential nutrients required for various cellular metabolic processes, including ATP production and DNA synthesis. However, iron can also act as a cancer-promoting factor by generating reactive oxygen species (ROS) through the Fenton reaction. Therefore, utilizing siderophores to chelate iron holds promise in targeting cancer cells and inhibiting their growth (Khasheii et al., 2021).

Deferasirox, a siderophore derivative from *Streptomyces pilosus*, has successfully cured a patient with chemotherapy-resistant acute monocytic leukemia. It has been reported that this remarkable cure was attributed to the inhibition of NFκB activity and the dephosphorylation of mTOR (Fukushima et al., 2011). In another study using mouse cell lines, the anticancer effectiveness of enterobactin was demonstrated, primarily attributed to its potent iron chelation ability (pFe=34.3). Interestingly, iron-free enterobactin exhibited cytotoxic effects against specific cancer cell lines, such as those derived from monocytes (RAW264.7 and J774A.1) (Saha et al., 2019).

1.2.5.3 Treatment for other types of diseases

Siderophores can also find applications in therapies beyond combating MDR bacteria. They have been investigated for their potential use in chemotherapy against malaria. Iron is crucial for the survival of all organisms, including malarial parasites. Studies have explored the use of reverse siderophores, known as "synthetic carriers," in this context. These reverse siderophores are designed to be more lipophilic, allowing them to enter cell membranes through diffusion. Once inside the cell, they scavenge intracellular iron, acting as *in vitro* growth inhibitors against various MDR strains of *Plasmodium falciparum*, without affecting mammalian cells in culture (Shanzer et

al., 1991). *In vivo* studies have shown that a synthetic siderophore called DFP-RVT (Deferiprone-resveratrol) exhibits high efficacy by inhibiting DNA synthesis and increasing oxidative damage in *Plasmodium* cells. This resulted in improved survival of mice infected with *Plasmodium berghei* (Chuljerm et al., 2021). Another study demonstrated the *in vitro* effectiveness of both natural and synthetic siderophores conjugated with the antimalarial agent 1,2,4-trioxolanes against MDR strains of *P. falciparum* (Tiwari et al., 2023).

Siderophores have also shown potential in the treatment of diseases associated with iron overload. In the 1970s, dfoB was utilized for the treatment of iron-overload diseases such as hemochromatosis and β-thalassemia (Wilson et al., 2016). This siderophore also has the ability to bind to aluminum, making it a potential treatment for aluminum toxicity following dialysis (Day and Ackrill, 1993). More recently, Deferasirox has emerged as a promising option not only for cancer therapy but also for the treatment of iron overload diseases. It has been demonstrated to be more effective than dfoB in patients with iron overload conditions, mainly due to improved patient compliance (Al-Kuraishy and Al-Gareeb, 2017). Deferiprone, which was investigated in the 1980s for the management of iron overload, resulted in significant side effects and is now considered as a treatment option only when dfoB or Deferasirox are not suitable (Codd, 2023). Table 1 provides a comparison of these three treatment options.

Table 1: Comparison of iron chelators derived from siderophores that are used in iron overload diseases. Characteristics based on the description by Al-Kuraishy and Al-Gareeb, 2017; Codd, 2023.

Treatments / Characteristics	dfoB	Deferasirox	Deferiprone
Year of FDA approval	1968	2005	2011
Structure	Large hydrophile hexadentate hydroxamate siderophore	Small tridentate ligand	Bidentate ligand
Ligand to iron ratio	1:1	2:1	3:1
Oral bioavailability	No	Yes	Yes
Medical dosage	Administered subcutaneously or intravenously five times a week	Administered orally once a day	Administered orally three times a day
Potential side-effects	Growth retardation and severe pain at site of injection	Transient acute renal insufficiency	Neutropenia and thrombocytopenia, arthropathy, gastric upsets and liver damage

2. Objectives

The aim of this Master's thesis is the characterization of a siderophore produced by *Pseudomonas graminis* LMG 21661^T.

A putative siderophore gene cluster was identified in the genome of *P. graminis* by genome mining. The **first objective** of this work is an *in silico* analysis, using online bioinformatic analysis tools, of the siderophore gene cluster to be able to obtain information about its structure.

The **second objective** of the work is to verify whether the genes of the siderophore gene cluster are indeed expressed under iron-limiting conditions and repressed by low amounts of iron as expected from a siderophore, by means of RT-qPCR. The effect of zinc on the expression is also investigated.

The **third objective** is the purification of the siderophore and LC-MS analysis. These results, in combination with the *in silico* analysis, can give a preliminary prediction of the structure of the siderophore.

Targeted genome screening of *Pseudomonas* genomes showed that the siderophore gene cluster was found in strains belonging to the *P. lutea* group of the *Pseudomonas* genus. For the **fourth objective** this is studied through the screening by LC-MS of a small collection of strains from the *P. lutea* group from an in-house collection for the production of the siderophore.

Pseudomonas strains are generally good competitors for iron because they have the ability to utilize iron complexes of a variety of different siderophores produced by other microorganisms, including fungi and bacteria. Genome analysis identified several strains with a putative receptor for the studied siderophore. For **objective five** it is studied if other *Pseudomonas* strains are able to utilize the studied siderophore by means of growth stimulation assays, and for one of these strains a receptor-negative mutant will be constructed to confirm the nature of the receptor.

For the **sixth objective** the antimicrobial properties of strains producing the siderophore and of the purified siderophore is studied on a panel of clinical strains.

All the strains producing the siderophore under study belong to one taxonomic group, the *P. lutea* group, which do not produce pyoverdine, a common siderophore produced by many *Pseudomonas* sp. Studies have shown that most *Pseudomonas* sp. can take up several pyoverdines. For the **last objective**, the ability of the strains of the *P. lutea* group to use pyoverdine(s) is assessed through growth stimulation assays with a large collection of pyoverdines.

3. Material and methods

3.1. Growth conditions

3.1.1 Medium cultures

3.1.1.1 Casamino acids medium (CAA)

Pseudomonas strains are cultured in CAA medium. This latter is an iron-poor medium used for routine cultures (5 g/l Bacto Casamino Acids (Difco Laboratories), 0.9 g/l K_2HPO_4, 0.25 g/l $MgSO_4.7H_2O$). For solid CAA, agar is added (15 g/l) (Cornelis et al., 1992).

For 2,2'-bipyridine agar, 2,2'-bipyridine is directly added to melted CAA cooled down to 60°C (concentration used is standardized for each *Pseudomonas* strain).

3.1.1.2 CAS agar medium

CAS (Chrome Azurol S) assay is a colorimetric assay where CAS is used to detect siderophore production due to the property of CAS to become yellow when a strong chelator removes the iron from the medium. For CAS agar (Schwyn and Neilands, 1987), the CAS solution is directly added to melted and cooled down to 60°C CAA (100 ml/l).

3.1.1.3 Minimal succinate medium (MSM)

For large-scale purification of siderophore, MSM was used. This is an extremely poor medium depleted of iron and composed of salts and succinate as carbon source (6 g/l K_2HPO_4, 3 g/l KH_2PO_4, 0.25 g/l $MgSO_4.7H_2O$, 1 g/l $(NH_4)_2SO_4$, 4 g/l succinic acid). The medium is adjusted at pH 7 with 5M NaOH (Vindeirinho et al., 2021).

3.1.1.4 In house 853 medium

When rich conditions are needed, the bacteria, as well as *C. albicans,* are cultured in 853 medium. This is a rich medium (not depleted in iron) composed of 10 g/l Bacto tryptone, 5 g/l yeast extract, 5 g/l NaCl, 1 g/l glucose, 0.7 g/l K_2HPO_4 and 0.3 g/l KH_2PO_4. For the solid medium, agar is added (15 g/l) (Matthijs et al., 2014).

3.1.2 Precultures conditions

All the *Pseudomonas* strains (Table 3) are taken from a petri dish (solid CAA) and inoculated in a sterile tube containing 6 ml of liquid CAA. The tube is then deposited on an agitation plate (200 rpm) and incubated at 30°C overnight. Similarly, the clinical strains (Table 4) are taken from 853 plates, inoculated in a sterile tube containing 6 ml of 853 medium and deposited on an agitation plate (200 rpm) at 37°C overnight.

3.2. *In silico* analyses

The siderophore gene cluster analyses were conducted using BLAST (https://www.ncbi.nlm.nih.gov), PKS/NRPS analysis (http://nrps.igs.umaryland.edu), Interpro (https://www.ebi.ac.uk/interpro) and antiSMASH (https://antismash.secondarymetabolites.org) online tools to identify and analyse the genes coding for proteins involved in siderophore biosynthesis and transport, and to help to predict the structure of the *P. graminis* siderophore.

3.3. Reverse transcription qPCR (RT-qPCR) analyses

To assess that the siderophore gene cluster found *in silico* is indeed expressed and regulated by iron or zinc RT-qPCR analyses were conducted. The studied genes were NRPS1 (*mrbD*), the first NRPS gene and rec1 (*mrbG*), the receptor gene. Therefore *P. graminis* LMG 21661^T was grown overnight in liquid CAA medium and 20 ml of the preculture, adjusted to OD_{660nm} = 0.2, was inoculated in 180 ml of liquid CAA and incubated at 30°C (200 rpm) till the OD_{660nm} reached 0.2. Then, the culture was divided into six subcultures (30 ml per flask) to study the effect of increasing iron concentrations. Therefore, the subcultures were supplemented with $FeCl_3$ to a final concentration of 0, 0.05, 0.1, 0.2, 0.5 and 0.7 µM $FeCl_3$ (Merck). Similarly, the effect of $ZnCl_2$ (Fisher Chemical) was studied using higher concentrations, 0, 0.5, 1, 2, 4 and 8 µM. These supplemented subcultures were then incubated for 1h at 28°C (200 rpm).

Subsequently, the subcultures were centrifuged, resuspended in fresh liquid CAA and RNAprotect Bacteria reagent (Qiagen) was added. The total RNA was extracted with RNeasy Mini kit (Qiagen). The samples were treated with RNAse free DNA Set (Qiagen) to eliminate putative presumptive genomic DNA contamination. The integrity of RNA was assessed by conducting a 10 % agarose gel electrophoresis (40 min – 100 V) and its purity and concentration were measured using a NanoDrop DeNovix DS-11 spectrophotometer (DeNovix Inc., Wilmington, DE USA).

Reverse transcription was done with 1 µg of RNA for each sample with RevertAid H Minus First Strand cDNA synthesis kit with oligo(dt) primers (Thermo Scientific). During this step, the "nRT" condition is established, wherein the samples are prepared without undergoing the reverse transcription reaction. This is achieved by excluding the nucleotides, primers, ribonuclease inhibitor, and reverse transcriptase from the reaction tubes. The purpose of this condition, conducted in parallel with the "RT" condition where all these components are present, is to specifically detect any pre-existing DNA in the samples. Consequently, if DNA is detected in the "nRT" tubes at the conclusion of the RT-qPCR, it signifies that the DNA was already present before the reaction commenced. Therefore, it needs to be subtracted from the "RT" reaction to eliminate background interference.

Before the RT-qPCR assays the cDNA was purified by means of the QIAquick PCR Purification kit (Qiagen). Quantification of the cDNA was conducted using Fast start Essential DNA Green Master (Roche Applied Science) and the appropriate primers (Table 2) on a LightCycler 96 (Roche).

Table 2: List of primers used for the study of biosynthesis and receptor genes as well as the investigation of reference genes.

Gene	Forward primer sequence	Reverse primer sequence
Nrps1	5'-AGCGACAACGAGCTGTTCA-3'	5'-TCCAGCGCCTGTTCGATGT-3'
Rec1	5'-AGCACCAGTTCAACGACA-3'	5'-TGCCAAAACCGGCGTTAT-3'
fabD	5'-GCGGTGAATTTCAATTCGC-3'	5'-GCCTTGCACACTTCGATG-3'
rho	5'-ACCGATCTGCTCGAAATGG-3'	5'-GAGATTTCCTCGCCGCTT-3'
rpoS	5'-GCTCTCAGCAAAGAAGTGC-3'	5'-TGCACGAACAGAAGGTGT-3'
rpoD	5'-GATTACCTTGGGTCGTGAG-3'	5'-GGATGATGTCTTCCACCTG-3'
nadB	5'-CCAGCACGACGTATTGGTA-3'	5'-CGTTCGCCAGATCACCTT-3'

To normalize the quantity of DNA, reference genes were chosen by considering specific criteria derived from the regression curve analysis. These criteria included a slope ranging from -3.2 to -3.5 (with -3.3 being the ideal value), an efficiency value closest to 2, and an R^2 value closest to 1. The slope of the regression curve indicates the rate of change in the amplification efficiency, the efficiency represents the effectiveness of the PCR amplification, and a higher R^2 value suggests a stronger correlation between the cycle threshold values and the concentration of the target gene. Additionally, the expression levels of the selected reference gene(s) were also compared to those of the genes of interest (*rec1* and *NRPS1*) to ensure comparability between them. Five candidates were investigated: *fabD* (malonyl CoA-acyl carrier protein transacylase), *rho* (transcription termination factor Rho), *rpoS* (RNA polymerase sigma RpoS), *rpoD* (RNA polymerase sigma factor RpoD) and *nadB* (L-aspartate oxidase). The appropriate primers are listed in Table 2. It is essential to select reference genes that are stably expressed under all the experimental conditions studied. This ensures that the expression level of the reference gene does not vary significantly, which could impair the results of the analysis.

To construct a standard curve, genomic DNA was extracted from *P. graminis* LMG 21661^T using the DNeasy Blood and Tissue Kit (Qiagen) from an 8 ml culture grown overnigth in 853 medium. The quantification of total DNA was carried out using the NanoDrop DeNovix DS-11 spectrophotometer (DeNovix Inc., Wilmington, DE, USA). To evaluate potential contamination with organic compounds and proteins, absorbance ratios at 230 nm, 260 nm, and 280 nm were measured. Furthermore, the standard curve was generated using five different dilutions of the genomic DNA. This standard curve serves as a reference for quantifying and analyzing the samples.

3.4. Purification and LC-MS analysis of the *P. graminis* LMG 21661^T siderophore

To purify the *P. graminis* siderophore 100 ml cultures were grown for 42–48 h at 30°C in 500 ml Erlenmeyers. Subsequently the cultures were centrifuged for 15 min at 10,000g, the supernatant was filtered with a 0.2 µm Minisart Satorius filter (Stedim Biotech) and applied to a CHROMABOND C18 ecf column (Macherey-Nagel) that was activated with methanol and washed with distilled water. Elution was done with acetonitrile/H_2O (70/30%). The masses of the siderophores were determined by LC-MS using an Alliance e2695 separation module equipped with a 2998 PDA detector (Waters, Milford, MA, USA) and coupled to an Altus SQ mass detector (Perkin Elmer) (ES ionization, positive mode, cone voltage 49 V, capillary voltage 3.1 kV, source temperature 150°C, desolvation temperature 600°C). The column is a C18 Altima (Grace) (250 x 4.6 mm, 10 µm) with a flow rate of 0.5 mL/ min and a gradient from H_2O/CH_3CN 9:1 containing 0.1% formic acid to H_2O/CH_3CN 3:7 containing 0.1% formic acid. Mass spectral data were collected and analyzed using Empower 3 software (Grosse et al., 2023).

3.5. Large-scale purification of the putative siderophore

To purify the putative siderophore, a large-scale purification is conducted which consists out of two major steps, first supernatant of *P. graminis* LMG 21661^T was run on a C18 column, thereafter the samples were further purified using preparative HPLC.

Therefore, three milliliters (10 x 3ml) from a *P. graminis* LMG 21661^T overnight preculture in 100 ml CAA were used to inoculate ten 4l Erlenmeyers with 1l of MSM. These Erlenmeyers were then incubated for 72h at 28°C (180 rpm).

The cultures were centrifuged for 30 min (4500 rpm) and the supernatant was passed through a CHROMABOND C18 ecf column (Macherey-Nagel) (2.5 x 4 cm) which was activated with methanol and subsequently rinsed with MQ water. After the passing of the supernatant the column was rinsed with MQ to remove salts. The putative siderophore was eluted using 100-200 ml 70% CH_3CN. The samples were filtered (0.2 µm sterilizing filters - Millisart), evaporated to concentrate the semi-purified siderophore and lyophilized. After lyophilization, the samples were resuspended in 4 ml MQ and filtered with a 0.2 µm Millisart filter.

CAS assay guided fractionation was done on the semi-purified sample using a Prep 150 LC system (Waters). A SunFire Prep C18 column (C-18, 19 x 250 mm, 5 µm particle size) was used with a flow rate of 20 ml/min and a gradient going from H_2O/CH_3OH 9:1 containing 0.1 % CF_3COOH to H_2O/CH_3OH 2:8 in 20 min. UV detection was performed at 220 nm.

The CAS-positive fractions were then analyzed by LC-MS to determine the *m*/z ratio and Rt (retention time) of major components in each fraction.

3.6. Screening of the strains of the *P. lutea* group for the putative siderophore production

3.6.1 Strains of the *P. lutea* group used in this study

The strains used in this study are provided in Table 3. To obtain a comprehensive understanding of the taxonomic relationships among these strains, a phylogenetic tree was constructed using the housekeeping gene *rpoD*. The resulting tree is presented in Annex I, offering a visual representation of the phylogenetic relationships between the strains.

Table 3: List of strains of the *P. lutea* group used in this study. NA: not available.

Strains	Accession number genome	Accession number siderophore gene cluster	Biological origin	Reference strain
***P. graminis* LMG 21661^T**	FOHW00000000.1	SAMN05216197_103143 - SAMN05216197_103132	Grasses, phyllosphere	BCCM/LMG
***P. graminis* P265/09**	NA	NA	Grasses, phyllosphere	Behrendt et al., 1999
***P. graminis* P334/03**	NA	NA	Grasses, phyllosphere	Behrendt et al., 1999
***P. graminis* P200/02**	NA	NA	Grasses, phyllosphere	Behrendt et al., 1999
***P. graminis* P294/05**	NA	NA	Grasses, phyllosphere	Behrendt et al., 1999
***P. graminis* W2Oct35**	NA	NA	River water	Matthijs et al., 2013
***Pseudomonas* sp. W2Oct36**	NA	NA	River water	Matthijs et al., 2013
***Pseudomonas* sp. W2-17**	NA	NA	River water	Matthijs et al., 2013
***P. lutea* LMG 21974^T**	JRMB000000001.1	LT42_01460 - LT42_01510	Grasses, rhizospheric soils	BCCM/LMG
***P. abietaniphila* LMG 20220^T**	FNCO01000001.1	SAMN05216605_10184 - SAMN05216605_10190	Aerated lagoon of bleached kraft pulp mill effluent	BCCM/LMG
***P. bohemica* LMG 30182^T**	NKHL00000000.1	SAMN05216605_107326 - SAMN05216605_107323	Engraver beetle	BCCM/LMG

3.6.2 CAS assay

To assess the putative production of the studied siderophore by strains of the *P. lutea* group (Table 3), siderophore production was first verified by CAS assay. Therefore, 5 µl of overnight CAA cultures (6 ml), adjusted at $5x10^6$ cells, are deposited on CAS agar, and incubated at 30°C. Lectures are done after 48h by measuring the yellow area around the colony representing the siderophore diffusion zone. Experiments were performed three times with four replicates each time.

3.6.3 LC-MS analyses

Subsequently the siderophores were purified as described above (refer to section *3.4. Purification and LC-MS analysis of the P. graminis LMG 21661^T siderophore*) and analyzed by LC-MS. *P. graminis* LMG 21661^T was used as a positive control, and *P. bohemica* LMG 30182^T as a negative control since the *P. graminis* siderophore gene cluster was absent from the genome. The gene cluster of the siderophore under study was identified in the genomes of *P. lutea* LMG 21974^T and *P. abietaniphila* LMG 20220^T (Table 3). For the other strains, the genome sequence was not available (Table 3).

3.7. Assessment of the *in vitro* antimicrobial activity of the *P. graminis* siderophore producing strains and purified siderophore fractions against a panel of clinical strains

3.7.1 Panel of clinical strains studied

Clinical strains investigated are listed in Table 4.

Table 4: List of clinical strains investigated in this study.

Strains	Gram	Strain reference	Pathogenicity in humans
***Staphylococcus capitis* I**	Positive	Isolated from the skin of a healthy patient (gift Flahaut – U.L.B.)	Most frequently: commensal flora Less frequently: prosthetic valve endocarditis, neonatal sepsis, and hospital-acquired meningitis (Cameron et al., 2015)
***Escherichia coli* DV 4951**	Negative	Isolated from a patient with diarrhea (gift Hernalsteens – V.U.B)	Intestinal flora Enteric diseases (diarrhea or dysentery), and extra-intestinal infections (urinary tract infections and meningitis) (Kaper et al., 2004)
***Salmonella enterica* subsp. *enterica* LMG 3264**	Negative	BCCM/LMG	Most frequently: gastroenteritis (foodborne illness) Less frequently: hepatomegaly and splenomegaly (Eng et al., 2015)
***Bacillus cereus* LMG 6910**	Positive	BCCM/LMG	Most frequently: gastroenteritis (foodborne illness) Less frequently: non-gastrointestinal-tract infections (severe eye infections, anthrax-like progressive pneumonia, sepsis, and central nervous system infections) (Bottone, 2010)
***Candida albicans* LMG 3731**	/ (Yeast)	BCCM/LMG	Most frequently: commensal flora Less frequently: skin infections or severe systemic infections in immunodeficient individuals (Mayer et al., 2013)
***Clostridium sporogenes* LMG 8421**	Negative	BCCM/LMG	Enteritis, cellulitis, and septicemia (Abusnina et al., 2019)
***Enterococcus hirae* LMG 10274**	Positive	BCCM/LMG	Most frequently: endocarditis and sepsis Less frequently: urinary tract infections (Bourafa et al., 2015)

***Pseudomonas aeruginosa* LMG 9009**	Negative	BCCM/LMG	Most frequent hospital-acquired infection Serious infections of almost any organ (lung, skin) in immunodeficient and immunocompetent individuals (Qin et al., 2022)

3.7.2 *In vitro* antagonism assay

To determine if any of the strains of the *P. lutea* group produce an iron-repressed molecule capable of inhibiting the growth of a panel of clinical strains (Table 4), cultures of the *Pseudomonas* strains (Table 3) were grown overnight in 6 ml liquid CAA. The cultures were adjusted at OD_{600nm} = 0.5 and 10 µl was inoculated in quadruplicates on 20 ml CAA plates and CAA plates + 100 µM iron and incubated at 28°C for 48h. The *Pseudomonas* strains were then killed using chloroform vapors (20 mins). After evaporation of the chloroform, a soft agar overlay (7.5 g/l agar) mixed with a clinical strain (Table 4) adjusted at OD_{600nm}= 0.5 in 853 media was prepared. Six ml of the overlay was uniformly overlaid on each plate on which the *Pseudomonas* strains had been killed with chloroform. After solidification of the top layer the plates were incubated overnight at 37°C.

Using a similar assay, the antimicrobial properties of purified siderophore fractions were evaluated against the same batch of clinical strains. A soft agar overlay was prepared as described above and overlaid on 20 ml 853 plates. After solidification, a sterile cork borer was used to cut wells in the agar. The obtained wells were filled with 100 µl of filtered (0.2 µm sterilizing filters – Millisart) siderophore fractions (purified by preparative HPLC). As control 70% CH_3CN was used. The plates were incubated overnight at 37°C.

3.8. Characterization of a putative siderophore piracy

3.8.1 Characterization of a siderophore receptor in non-producing *Pseudomonas* strains

BlastX analysis of the studied siderophore receptor identified many *Pseudomonas* strains with a putative receptor. Of six of these strains siderophore-negative mutants (Table 5) were present in the in-house *Pseudomonas* collection. For these strains it was verified by means of growth stimulation assays using the purified *P. graminis* siderophore whether the siderophore mutants were able to utilize it.

Table 5: List of siderophore-negative *Pseudomonas* mutants with a putative *P. graminis* siderophore receptor.

Mutant name	Mutant characteristics	Reference strain
Prho^{T}ΔpvdLΔtrbABC-44	Pyoverdine and triabactine-negative deletion mutant of *P. rhodesiae* LMG 17764^T	Matthijs and Brandt, *unpublished*
WCS417-M634	Pyoverdine-negative Tn5 of *P. simiae* WCS417r, predicted to produce mupirochelin	Duijff et al., 1993
WCS358-JM213	Pyoverdine-negative Tn5 mutant of *P. putida* WCS358	Marugg et al., 1985
WCS374-BT1	Pyoverdine, pseudomonine and salicylic acid-negative Tn5 mutant of *Pseudomonas sp.* WCS374r	De Vleesschauwer et al., 2008; Djavaheri et al., 2012
SBW25-9H6	Pyoverdine and ornicorrugatin-negative Tn5 mutant of *P. fluorescens* SBW25	Matthijs and Brandt, *unpublished*
Pazo^T::pvdL32	Pyoverdine-negative Tn5 mutant of *P. azotoformans* LMG 21611^T	Matthijs and Brandt, *unpublished*

In this assay the strain to be tested (Table 5) is inoculated under iron-limiting conditions imposed by the chelator 2, 2'-bipyridine. The concentration of 2, 2'-bipyridine is high enough so that the strain cannot grow (very well). The siderophore to be tested is put on the media by means of a siderophore loaded Whatman paper disk. The siderophore will diffuse into the media. If the strain has the putative receptor for it, it can utilize the siderophore and grow around the disk. If the strain does not have the receptor it cannot grow. The assay is done with siderophore-negative mutants since the production of their own siderophore(s) would blur the results. To determine the optimal concentration of 2, 2'-bipyridine for each mutant, a panel of concentrations from 100 to 500 µM 2, 2'-bipyridine was tested. The optimal concentration represents the one at which no or hardly any background growth is observed.

P. bohemica LMG 30182^T does not have the gene cluster for the biosynthesis of the *P. graminis* siderophore, but it does have a putative receptor (Figure 17). To test the uptake of the siderophore by *P. bohemica* LMG 30182^T a growth stimulation assay was also performed with this strain.

3.8.2 Construction of a siderophore receptor mutant TWR49273 in *P. rhodesiae* LMG 17764^T

To confirm that the putative siderophore receptor found *in silico* is in fact the receptor for its uptake, the receptor gene was deleted in a *P. rhodesiae* LMG 17764^T siderophore-negative mutant. In this mutant the pyoverdine biosynthetic gene *pvdL* coding for the chromophore and the complete triabactin operon were deleted (Prho^{T}ΔpvdLΔtrbABC-44). This mutant was selected because it had clean deletions without antibiotic resistance markers and the strain was easy to mutagenize.

For the construction of the mutant the plasmid pME-TWR49273 was already made. Plasmid pME-TWR49273 was then integrated into the chromosome of Prho^{T}ΔpvdLΔtrbABC-44 by triparental

mating using *E. coli* HB101/pME497 as the mobilizing strain, with selection for tetracycline and chloramphenicol resistant recombinants. Excision of the vector through a second crossing-over event took place following the enrichment of tetracycline-sensitive cells (Schnider-Keel et al., 2000). The obtained mutant was confirmed by PCR amplification and sequencing using amplification primers. The method is detailed in Matthijs et al., 2016.

Growth stimulation assays are then performed on the new mutant (Prho^{T}ΔpvdLΔtrbABC-44ΔTWR49273) using purified siderophore fractions as described above.

3.8.3 Utilization of exogenous pyoverdines by strains of the *P. lutea* group

To assess if the *P. lutea* group strains have pyoverdine receptors, growth stimulation assays were performed with a collection of sixty pyoverdines (Table 6).

Twenty milliliter CAA agar plates containing 100 or 200 µM 2,2'-bipyridine were overlaid with $5x10^{6}$ cells of the strains of the *P. lutea* group (Table 3), and filter-paper disks impregnated with 5 µl of 32 mM purified pyoverdine were placed on the agar. The plates were incubated at 30°C and scored for the presence of detectable growth around the disk of the *Pseudomonas* strain after 1 and 2 days.

Table 6: List of *P. lutea* group strains with investigated pyoverdines. More details on studied pyoverdines are available in Annexes (Annex II).

Strains	Studied pyoverdines
***P. graminis* LMG 21661^{T}**	PYO_{PkilT}, PYO_{GB-1}, PYO_{G173}, $PYO_{W15Oct28}$, $PYO_{Pfl1.3}$, PYO_{L1} $PYO_{W2Jun44A}$, PYO_{cosT}, PYO_{90-136}, PYO_{PutC}, PYO_{BTP1}, PYO_{Pflii}, PYO_{PL8}, $PYO_{typeIII}$, PYO_{typeI}, PYO_{TolT}, PYO_{G176}, PYO_{G85}, PYO_{Gwose}, PYO_{G76}, PYO_{G400}, $PYO_{D-TR133}$, PYO_{90-44}, PYO_{PbreT}, PYO_{cedT}, PYO_{SalT}, PYO_{lurT}, PYO_{lurT}, PYO_{putT}, PYO_{GS43}, PYO_{BTP2}, $PYO_{DSM50106}$, PYO_{GS37}, PYO_{G24}, PYO_{aspT}, PYO_{51W}, PYO_{NCIMB}, PYO_{2908}, PYO_{citT}, PYO_{azoT}, PYO_{Pf0-1}, PYO_{Ps6-10}, PYO_{PL9}, PYO_{Pfl12}, $PYO_{Pf17400}$, PYO_{G4R}, $PYO_{W15Oct11}$, PYO_{rho}, PYO_{thiT}, PYO_{agaT}, $PYO_{Pfl18.1}$, $PYO_{W15Aug1}$, $PYO_{W15Apr2}$, PYO_{typeII}, PYO_{A6}, PYO_{Lille1}, PYO_{Pf-5}, PYO_{LBSA1}, PYO_{L48T} & PYO_{fulT}
***P. graminis* P265/09**	
***P. graminis* P334/03**	
***P. graminis* P200/02**	
***P. graminis* P294/05**	
***P. graminis* W2Oct35**	
***Pseudomonas sp.* W2Oct36**	
***Pseudomonas sp.* W2-17**	
***P. lutea* LMG 21974^{T}**	
***P. abietaniphila* LMG 20220^{T}**	
***P. bohemica* LMG 30182^{T}**	

4. Results

4.1. A gene cluster in *P. graminis* LMG 21661^T codes for a putative siderophore

Colonies of *P. graminis* LMG 21661^T produce a yellow halo on CAS plates indicative of siderophore production (Figure 10).

Figure 10: Colony of *P. graminis* LMG 21661^T on CAS agar showing siderophore activity by the yellow halo around it.

When analysing the genome of *P. graminis* LMG 21661^T for siderophore-mediated iron acquisition systems a putative gene cluster for a NRPS siderophore was identified. The gene cluster resides on a 37.5 kb fragment and includes 11 open reading frames (ORFs) (Figure 11). In the frame of this Master's thesis the genes of the gene cluster were named 'mrb'.

Figure 11: Putative gene cluster of a NRPS siderophore found in *P. graminis* LMG 21661^T.

The assignment of the predicted function for each ORF involved comparing the translated product with known proteins in public databases and conducting analysis using InterPro (Annex III). It revealed the presence of a sigma regulator, an ABC transporter, an L-ornithine N5-oxygenase, two NRPSs, a diaminobutyrate aminotransferase, a TonB-dependent receptor, a MbtH-like protein, a taurine dioxygenase, a formyl transferase and a ferric iron reductase. The gene cluster contains therefore the necessary information for the regulation, biosynthesis, and transport of a NRPS siderophore.

The presence of two NRPSs are predicted to assemble a peptide backbone. Based on online tools, a prediction of the length and composition of the peptide is possible based on the domains of NRPS multimodular enzymes (Table 7). The first domain of the predicted MrbD protein presented homology with members of the fatty acyl-AMP ligase family (FAAL, cd05931, e = 0) (Figure 11). This domain was characterized to activate and introduce long chain fatty acids in both polyketide and NRPS peptide biosynthesis by activation and loading of fatty acids to ACP domains (Patil et al., 2021). The presence of this domain led to the hypothesis that the siderophore is a lipopeptide siderophore.

In total six classical NRPS modules (C-A-T) were found, two in **MrbD** and four in **MrbE**, which indicates that probably a 6-residues long peptide backbone is produced. Using online prediction tools, the NRPS adenylation domain specificity and the D and L-forms of the residues (based on epimerization domains) was predicted (Table 7) resulting in an Asp – Dab – Ser – (Fo-)OH-Orn – Ser – (Fo-)OH-Orn backbone whereby the D-forms are underlined.

Table 7: NRPS adenylation domain specificity prediction using antiSMASH. X = unassigned residue.

Module	PKS/NRPS	Nearest Stachelhaus code	8Å match	Stachelhaus code match
MrbD				
1	D-Asp	DLTKIGHVGK	88%	100% (strong)
2	Dab	DIWELTADDK	88%	100% (strong)
MrbE				
1	D-Ser	DVWHVSLIDK	97%	100% (strong)
2	X = Fo-OH-Orn X = OH-Orn	DGEVCGGVTK DGEACGGVTK	74% 71%	80% (moderate)
3	Ser	DVWHVSLIDK	97%	100% (strong)
4	X = Fo-OH-Orn X = OH-Orn	DGEVCGGVTK DGEACGGVTK	74% 71%	80% (moderate)

Two non-proteinogenic amino acids are predicted to be found in the peptide chain of the siderophore (Table 7): Dab and (Fo-)HO-Orn. The L-Dab (2,4-diaminobutanoic acid) residue is probably produced from aspartate *ß*-semialdehyde by the enzyme diaminobutyrate-2-oxoglutarate transaminase (**MrbF**). L-ornithine N5-oxygenase (**MrbC**) catalyzes the conversion of L-ornithine to N_5-hydroxyornithine. Software could not really make a difference between non or formylated hydroxyornithine. Most likely the HO-Orn was in the formalyted form. The prediction of this residue was a bit better, and an acyltransferase (**MrbJ**) was found in the gene cluster. These modifications lead to the formation of the iron-chelating hydroxamate functional groups.

In addition, a thioesterase (TE) domain which catalyzes the release of the NRPS product was found in the last protein **MrbE** (Table 7). In the gene cluster a MbtH-like protein **MrbH** was found, many NRPSs require MbtH-like proteins for the proper folding, stability, and activity of the NRPS.

The last gene, *mrbK*, codes for a protein that is homologous to FhuF, the putative *E. coli* iron-ferrioxamine B reductase which is proposed reductively release ferrous iron from ferric-siderophore complexes. **MrbK** thus likely makes iron bound to internalized ferric-siderophore available.

The uptake of the siderophore probably occurs through the TonB-dependent receptor **MrbG** (Annex III).

4.2. *P. graminis* siderophore production is regulated by iron and not by zinc

4.2.1 Reference gene investigation

In this study, five reference genes (Figure 12) were examined to determine suitable candidate(s) for normalizing the expression of *rec1* and *NRPS1* genes. Among the studied reference genes, the *nadB* gene (Figure 12B) was selected based on the quality of its regression curve, as indicated by its slope, efficiency, and R^2 values (Figure 12F) reflecting a more accurate and reliable normalization factor. Furthermore, the expression levels of the reference genes were assessed by determining the cycle at which the first concentration surpasses the detection threshold. Ideally, this cycle should occur around the fourteenth cycle. The *nadB* gene exhibited expression levels that meet this criterion.

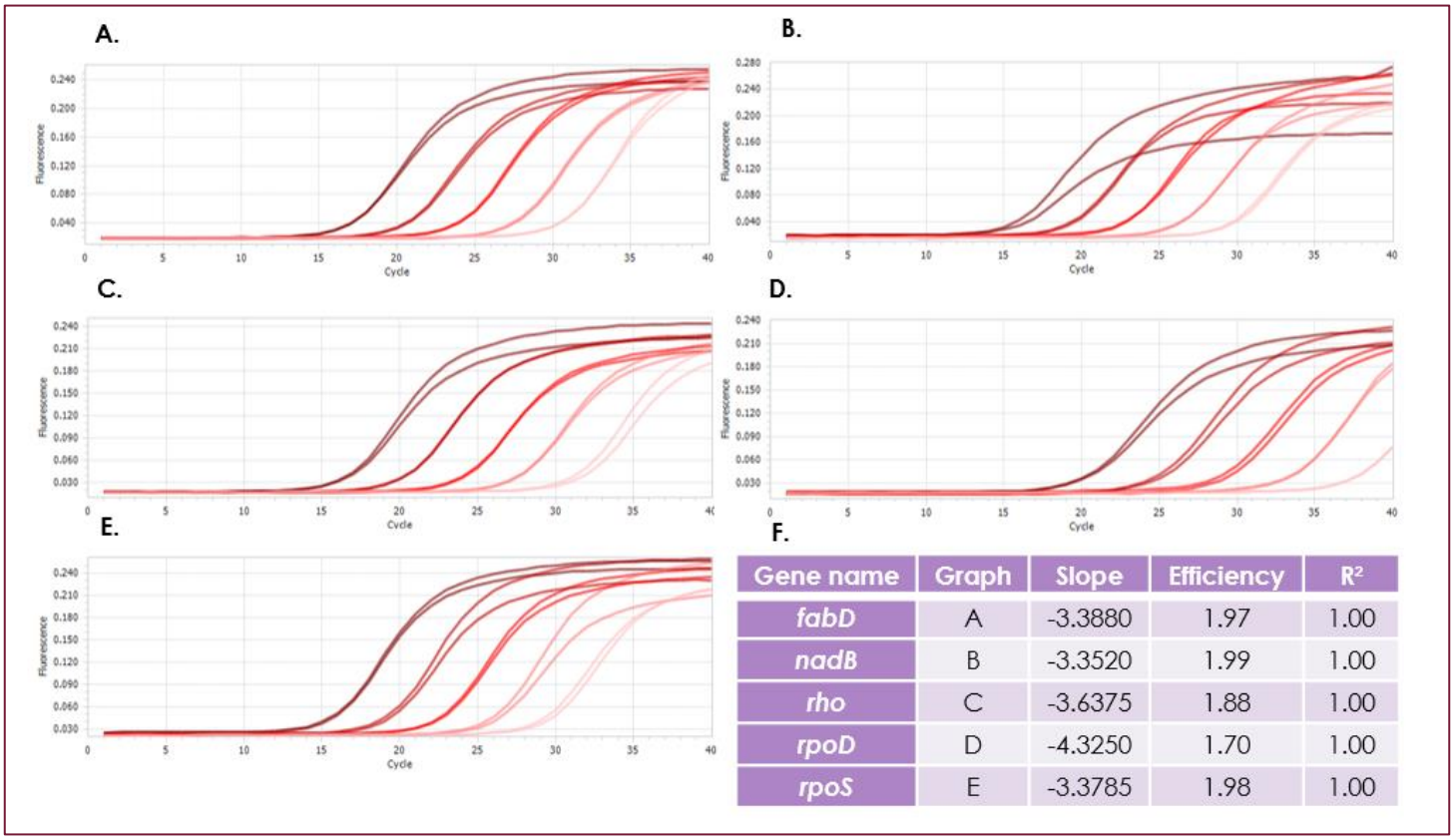

Gene name	Graph	Slope	Efficiency	R^2
fabD	A	-3.3880	1.97	1.00
nadB	B	-3.3520	1.99	1.00
rho	C	-3.6375	1.88	1.00
rpoD	D	-4.3250	1.70	1.00
rpoS	E	-3.3785	1.98	1.00

Figure 12: Fluorescence intensity profiles of standard DNA at various concentrations using investigated reference gene primers in duplicates. The concentrations used include 100,000-fold, 10,000-fold, 1,000-fold, 100-fold, and 10-fold dilutions. The investigated reference gene primers used in the study are labeled as follows: **A.** *fabD*, **B.** *nadB*, **C.** *rho*, **D.** *rpoD*, and **E.** *rpoS*.**F.** Quality of each regression curve is represented.

4.2.2 Biosynthesis and receptor gene expression based on Fe and Zn concentrations

Experiments were conducted at least two times for each metal and expression of *rec1*, the TonB-dependent receptor and *NRPS1*, the first NRPS gene, are presented as relative to the *nadB* reference gene.

RT-qPCR analyses showed that both expressions of *rec1* and *NRPS1* are not influenced by Zn (Figure 13B). Additionally, *rec1* and *NRPS1* expression is strongly repressed when Fe levels increase (Figure 13A), at a concentration of 0.1 µM $FeCl_3$ the siderophore biosynthesis is completely repressed, at a concentration of 0.1 µM the expression of the receptor is strongly repressed, at 0.5 µM it is completely repressed.

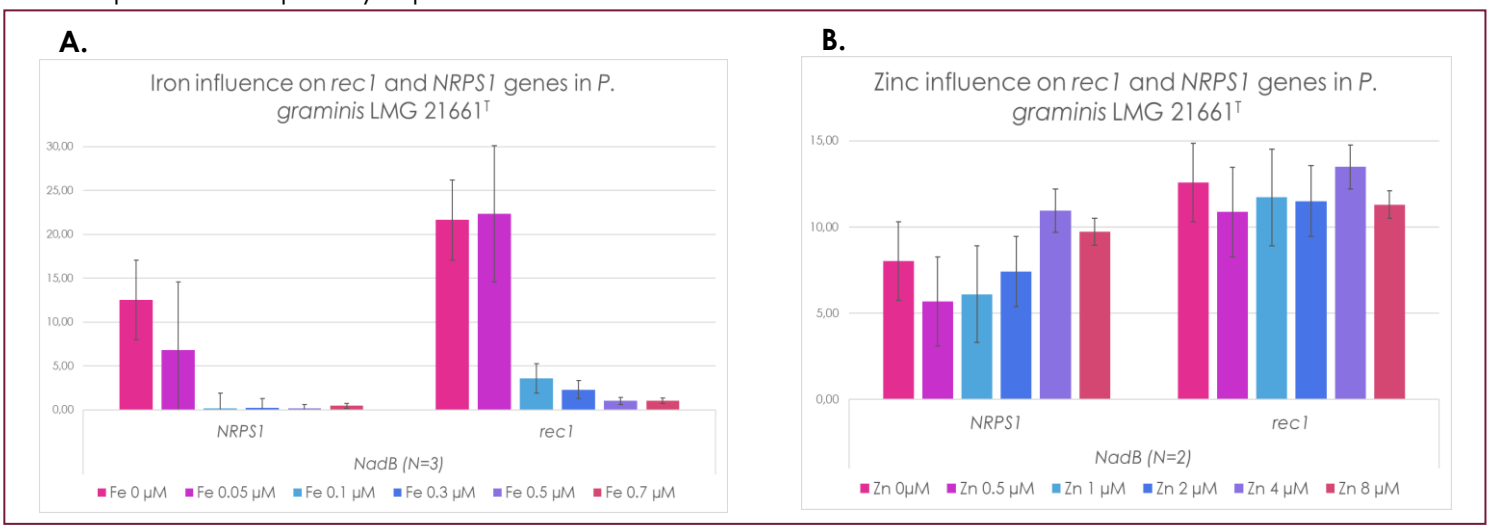

Figure 13: Expression of *rec1* and *NRPS1* genes depending on **A.** Fe and **B.** Zn concentrations relative to housekeeping gene *nadB*. For the study of iron influence, triplicates have been performed while for the study of zinc influence duplicates have been performed.

4.3. The *P. graminis* siderophore is produced as a suite of siderophores

4.3.1 Identification of the peaks with CAS activity

Ten liters of *P. graminis* supernatant was first purified on a large C18 column, subsequently the sample was purified by preparative HPLC which allows to separate molecules based on their differences in hydrophobicity. Several fractions corresponding to six distinct peaks eluting with retention times spanning 12–17 min had a siderophore activity based on CAS assay (Figure 14).

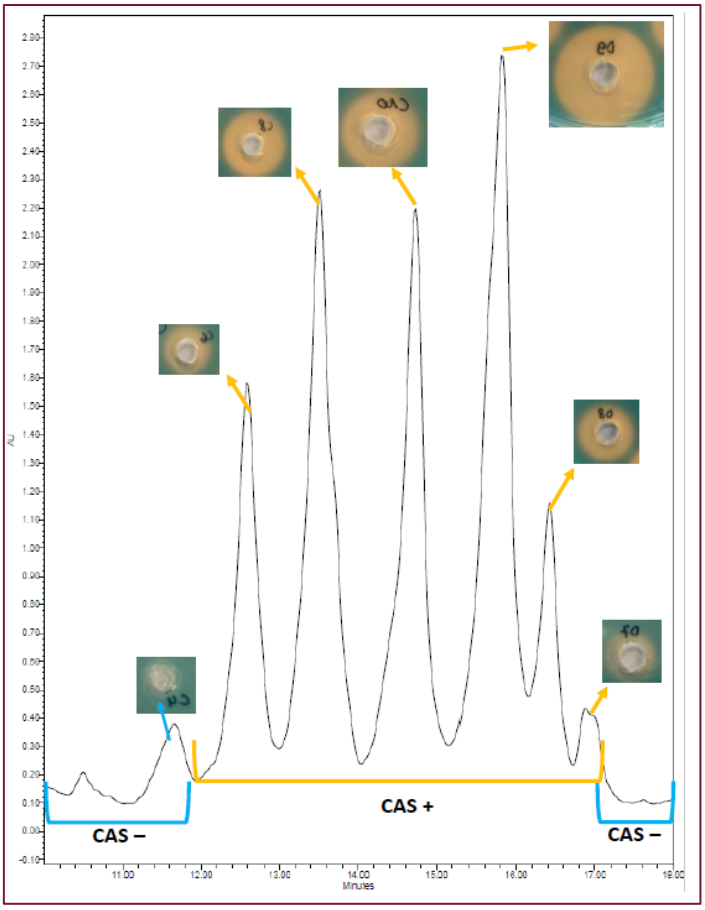

Figure 14: Chromatogram of *P. graminis* LMG 21661^T culture supernatant (220 nm). Each fraction has been tested for siderophore activity in CAS agar.

4.3.2 Determination of the *m/z* of the CAS-positive fractions

Injection of CAS-positive fractions in LC-MS allowed to determine the *m/z* of the major molecule in each peak. The results are shown in Table 8.

Table 8: CAS-positive purified fractions from HPLC and the characteristics of their major molecule.

CAS-positive Peak	Rt (min)	*m/z*
1st peak	20.722	874.70
2nd peak	21.718	876.70
3rd peak	23.522	902.72
4th peak	25.155	904.72
5th peak	26.494	930.74
6th peak	28.742	932.76

Based on the identified *m/z* values, it is evident that the major molecules in each peak represent closely related masses, suggesting the presence of various adducts or variants. Specifically, these variants could have hydrocarbon chains that are probably two methylene groups (Δ: 28.0307 Da, C_2H_4) shorter (Table 8). Additionally, the mass difference of 2 Da (Δ: 2 Da, 2H) (Table 8) could indicate variations in the degree of saturation of the fatty acid tails. These results indicate that probably a suite of siderophores is produced that exhibit differences in their fatty acid tails.

4.3.3 Prediction of the studied siderophore structure

The prediction of the peptide head group of the *P. graminis* siderophore (Figure 15A) is the same as the peptide head group of marinobactins produced by *Marinobacter* sp. DS40M6 (Martinez et al., 2000; Martinez and Butler, 2007). In addition, the genetic organization of the *P. graminis* gene cluster (Figure 15B) shows strong similarities to the marinobactin gene cluster of *Marinobacter* sp. DSM40M6 (Figure 15B). The genetic organization of the gene cluster of marinobactin is almost identical to the one of *P. graminis,* except for two genes involved in transport which are not present in the *P. graminis* gene cluster (Figure 15B).

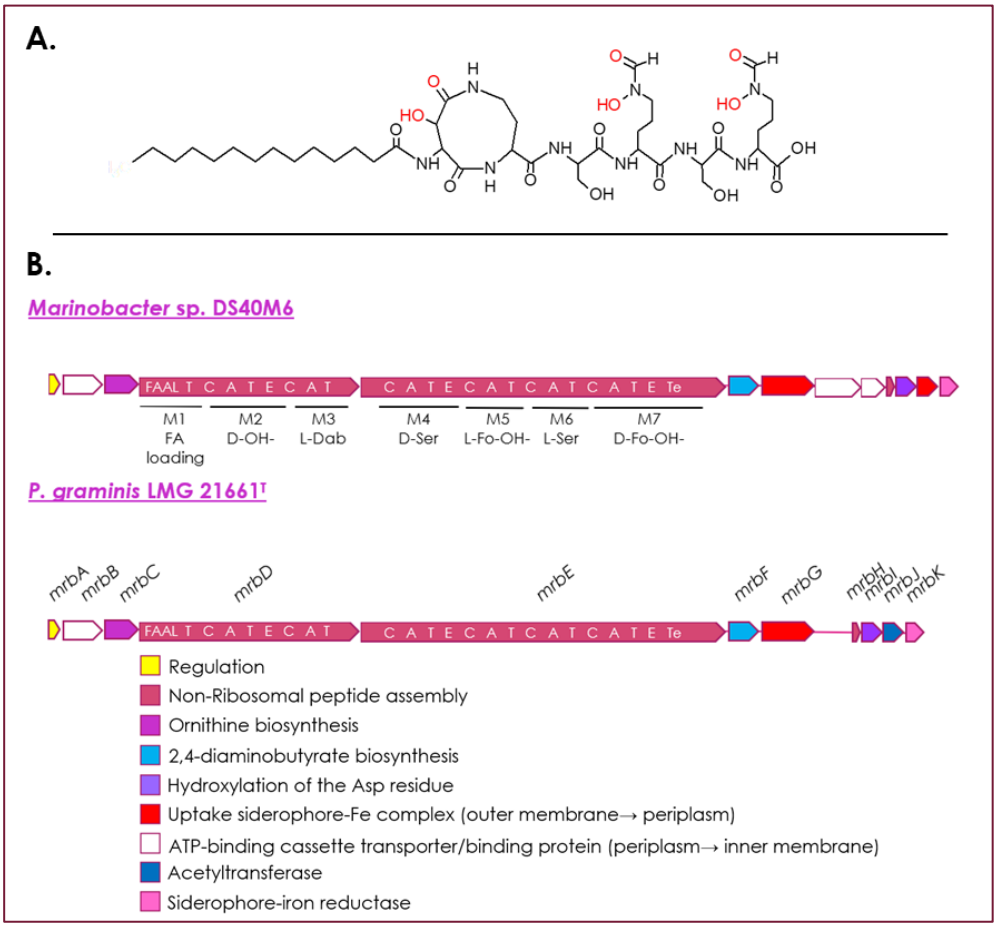

Figure 15: **A.** The structure of marinobactin A produced by *Marinobacter* sp. DS40M6 and predicted to be produced by *P. graminis* LMG 21661^T. The iron chelation moieties are indicated in red. **B.** Schematic presentation of the marinobactin biosynthetic and uptake operon of *Marinobacter* sp. DS40M6 and *P. graminis* LMG 21661^T. Gene names are indicated above the arrows. The organization of the modules and domains of the two NRPS, MrbD and MrbE, is shown on the arrows. C: condensation domain, A: adenylation domain, T: thiolation, E: epimerization domain. Predicted genes functions obtained by BLASTp and InterPro analyses: *MrbA*: RNA polymerase sigma-70 factor, ECF subfamily, *MrbB*: putative ATP-binding cassette transporter, *MrbC*: L-ornithine N5-oxygenase, *MrbD*: non-ribosomal peptide synthase, *MrbE*: non-ribosomal peptide synthase, *MrbF*: diaminobutyrate aminotransferase, *MrbG*: TonB-dependent receptor, MrbH: MbtH-like protein, MrbI: Taurine dioxygenase, MrbJ: Formyl transferase and MrbK: Ferric iron reductase.

But lower *m/z* values than the ones of marinobactin were observed for the *P. graminis* siderophore, only the MW of marinobactin A (932.0) was detected in the *P. graminis* sample. This could be explained by smaller acyl chains in the *P. graminis* siderophore (Figure 16, yellow square). Based on these results it is hypothesized that the *P. graminis* siderophore is marinobactin A and new variants with a shorter acyl chain in an unsaturated and saturated form.

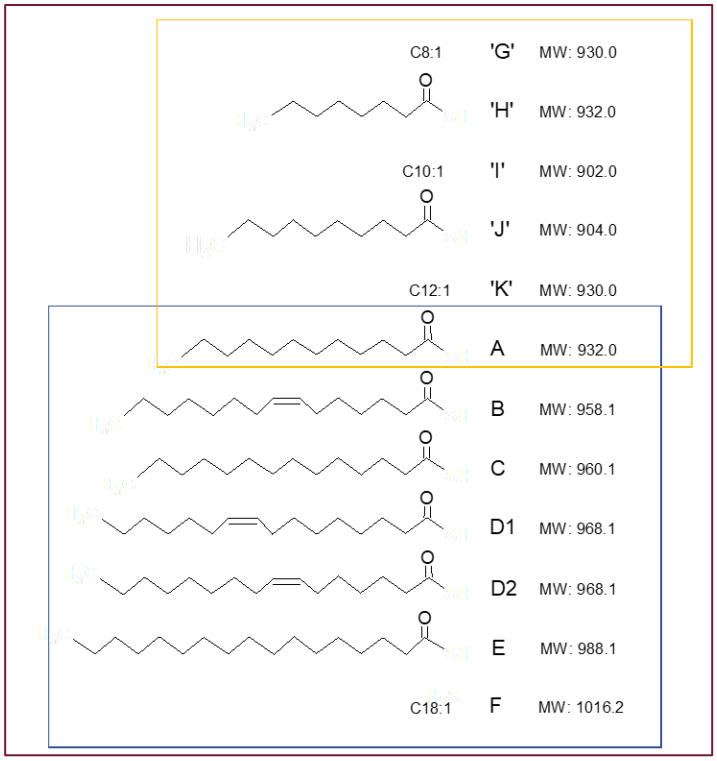

Figure 16: Structures of the fatty acid tails of marinobactins. The fatty acids in the blue square are marinobactin produced by *Marinobacter* sp. DS40M6. The fatty acids in the yellow square are predicted to be produced by *P. graminis* LMG 21661^T. Since the structures are predictions the codes of the fatty acid tails are between quotation marks. When the location of the double bond was not determined the fatty acid was not drawn.

4.4. The predicted marinobactin siderophore is the typical siderophore of strains of the *P. lutea* group

The strain *P. graminis* belongs to the *P. lutea* group. This group consists currently out of five members: *P. graminis*, *P. lutea*, *P. abietaniphila*, *P. harudinis* and *P. bohemica*. To investigate whether more strains of the *P. lutea* group produce the studied siderophore, siderophore production of three additional type strains, *P. lutea*, *P. abietaniphila*, and *P. bohemica,* and six strains from our in-house *Pseudomonas* collection (Table 3) was studied (Figure 17).

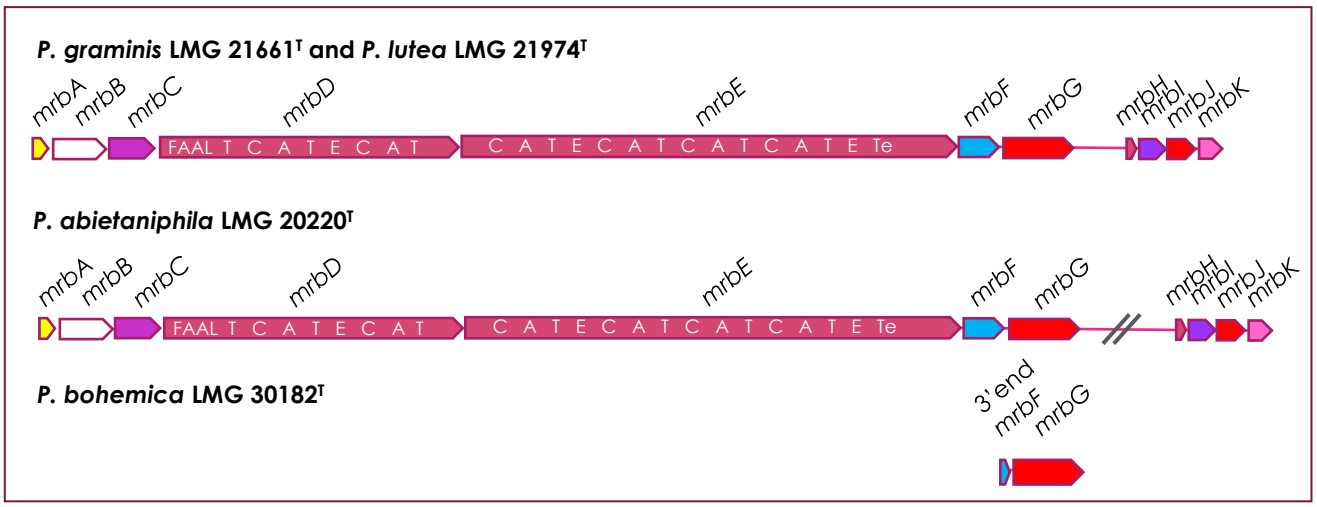

Figure 17: The putative marinobactin gene clusters of the type strains of *P. graminis*, *P. lutea*, *P. abietaniphila,* and *P. bohemica*. For *P. bohemica* only the putative marinoabactin receptor is present in the genome.

The type strains of *P. lutea* and *P. abietaniphila* have the siderophore gene cluster, in contrast to *P. bohemica* which has only the putative siderophore receptor, in their genomes. For the other strains (Table 3) no genome sequence was available.

4.4.1 CAS assays

To verify whether all strains (Table 3) produce predicted marinobactin, the siderophore production of the strains was verified through the CAS assay. The results show that all the studied *P. lutea* group strains are siderophore producers since yellow halos around the colonies have been observed for all strains (Figure 18). The size of the radius of the yellow halo showed great differences with *P. lutea* LMG 21974^T having the largest halo and *P. bohemica* LMG 30182^T having the smallest halo.

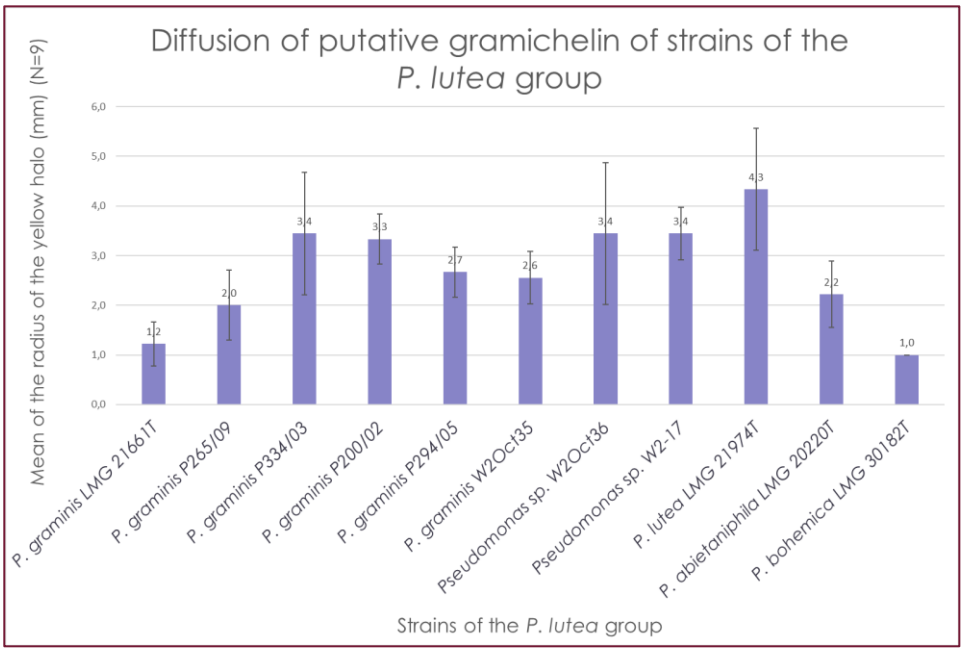

Figure 18: Evaluation of siderophore diffusion in CAS agar for each strain of *P. lutea* group. Measures have been obtained by measuring the radius of the yellow area around the strain colonies.

4.4.2 LC-MS analyses

LC-MS analysis of the supernatant of the *Pseudomonas* strains showed that all the *Pseudomonas* strains of the *P. lutea* group (Table 3), except for *P. bohemica* LMG 30182^T which does not have the biosynthesis genes, produce the predicted marinobactin. The same *m/z* values were observed as detected in *P. graminis* sample.

4.5 Several *Pseudomonas* sp. have a TonB-dependent receptor for the *P. graminis* siderophore

4.5.1 Siderophore-negative mutants with a putative marinobactin receptor in their genome can take up the *P. graminis* siderophore in an iron-restricted environment

BlastX analysis with the *P. graminis* receptor identified several strains that had a putative *P. graminis* siderophore receptor in their genome (but not the biosynthetic genes). To verify whether some of these strains can take up the *P. graminis* siderophore growth stimulation assays were carried out with siderophore-negative mutants of a few of these strains (Table 5). The tested strains were following: *P. bohemica* LMG 30182^T and six siderophore-negative mutants (Table 5) including *P. rhodesiae* Prho^{T}ΔpvdLΔtrbABC-44 (Figure 19A), *P. simiae* WCS417-M634 (Figure 19B), *P. capeferrum* WCS358-JM213 (Figure 19C), *Pseudomonas* sp. WCS374-BT1 (Figure 19D), *P. fluorescens* SBW25-15F3 (Figure 19E), and *P. azotoformans*^{T} ::pvdL32 (Figure 19F). Growth stimulation assays with fractions of the *P. graminis* siderophore (Table 8) showed that each mutant strain was able to grow around the siderophore loaded disk (Figure 19), but not if the siderophore was not supplemented (Table 9).

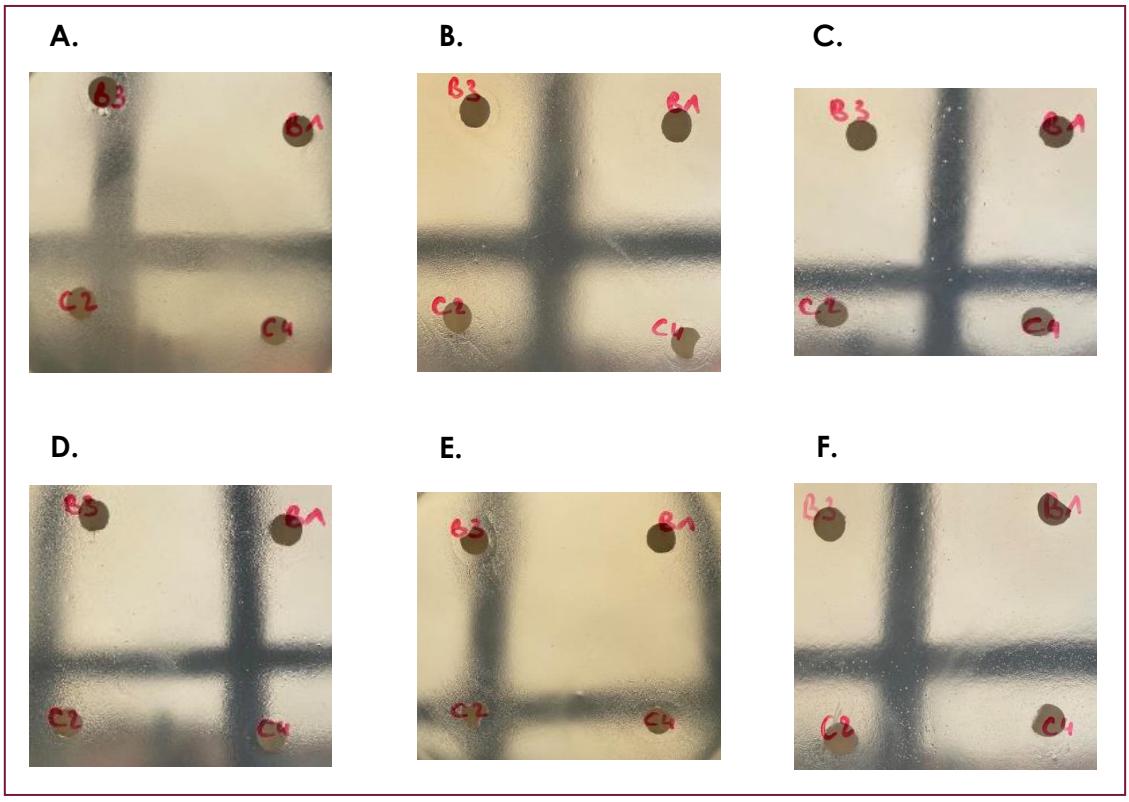

Figure 19: Growth stimulation assays of siderophore-negative mutants with fractions of *P. graminis* siderophore. **A.** *P. rhodesiae* Prho^{T}ΔpvdLΔtrbABC-44. **B.** *P. simiae* WCS417-M634. **C.** *P. capeferrum* WCS358-JM213. **D.** *Pseudomonas* sp. WCS374-BT1. **E.** *P. fluorescens* SBW25-15F3. **F.** *P. azotoformans*^{T}::pvdL32. **Abbreviations**: B3 = *m/z* 874.70, B1 = *m/z* 876.70, C2 = *m/z* 902.72 and C4 = *m/z* 904.72.

P. bohemica LMG 30182^T was not able to grow (Table 9) demonstrating that the putative *P. graminis* siderophore receptor is not functional in the conditions used (data not shown).

Table 9: Growth stimulation assays of *P. bohemica* LMG 30182^T and the six siderophore-negative mutants with fractions of the *P. graminis* siderophore as well as their optimal concentrations of 2, 2'-bipyridine.

Strain/Mutants	Optimal [2, 2'-bipyridine] (µM)	Fraction *m/z* 874.70	Fraction *m/z* 876.70	Fraction *m/z* 902.72	Fraction *m/z* 904.72	W/o any fraction
Prho^{T}ΔpvdLΔtrbABC-44	500	+	+	+	+	-
WCS417-M634	500	+	+	+	+	-
WCS358-JM213	500	+	+	+	+	-
WCS374-BT1	500	+	+	+	+	-
SBW25-6H9	400	+	+	+	+	-
Pazo^T::pvdL32	500	+	+	+	+	-
***P. bohemica* LMG 30182^T**	400-500	-	-	-	-	-

4.5.2 Construction of the receptor mutant ΔTWR49273 in *P. rhodesiae* LMG 17764^T

To verify whether the growth stimulation of the siderophore-negative mutants (see previous point) was indeed due to the identified TonB-dependent receptor a receptor-negative mutant was constructed for one of these strains, the siderophore-negative mutant Prho^{T}ΔpvdLΔtrbABC of *P. rhodesiae* LMG 17764^T. To obtain the mutant a markerless genomic deletion method by homologous recombination was used to achieve an in-frame deletion of the TonB-dependent receptor TWR49273.

After conjugation and tetracycline-enrichment five putative mutants were obtained. The deletion of the almost complete TWR49273 gene was verified by PCR amplification of the region before and after the deletion. Compared to the double mutant Prho^{T}ΔpvdLΔtrbABC-44 whose PCR amplification gave a fragment of approximately 4000 bp (Figure 20A) the triple mutant Prho^{T}ΔpvdLΔtrbABCΔTWR49273 gave a PCR fragment of approximately 2000 bp (Figure 20B) showing the loss of the TWR49273 gene. The amplicons obtained for mutants 159, 211, and 241 were sequenced. The results of the sequencing confirmed the deletion for the three mutants. Mutant Prho^{T}ΔpvdLΔtrbABCΔTWR49273-159 was used for further characterisation.

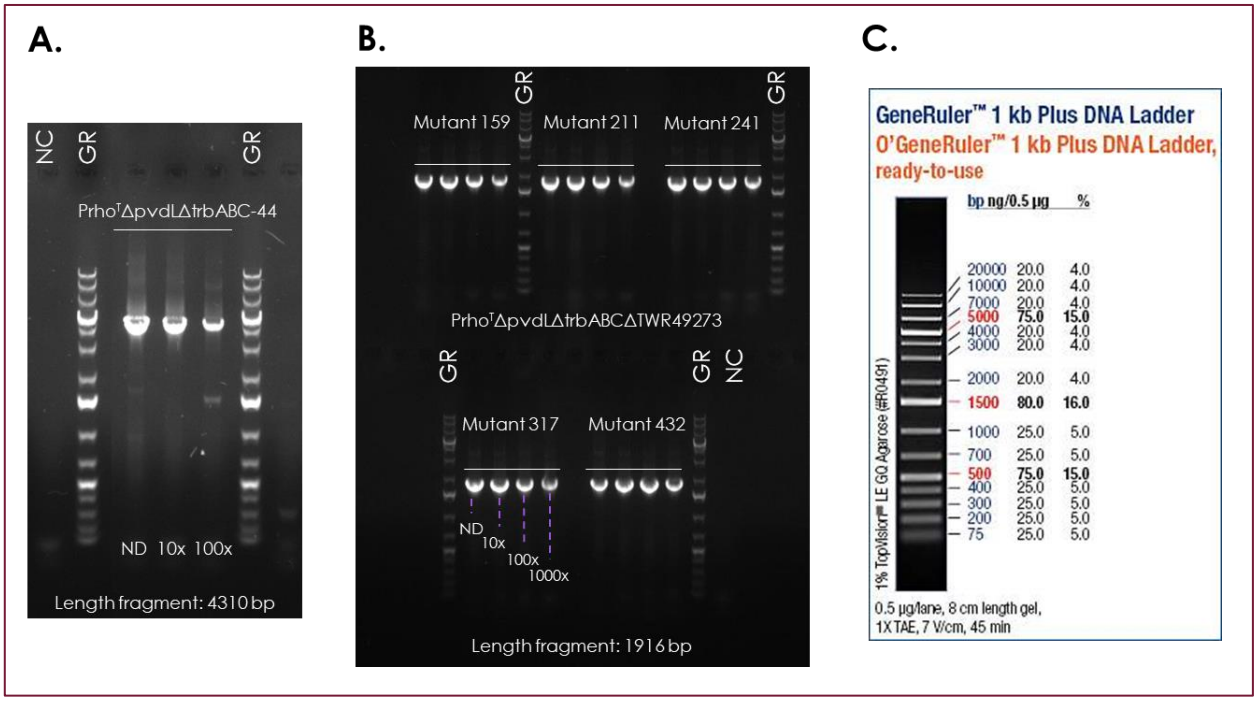

Figure 20: Confirmation PCR of the TWR49273 gene deletion. **A.** Electrophoresis gel of the double mutant PrhoTΔpvdLΔtrbABC-44 with a DNA length fragment of 4310 bp. **B.** Electrophoresis gel of the five triple mutants PrhoTΔpvdLΔtrbABCΔTWR49273 obtained (159, 211, 241, 317, and 432). **C.** Gene ruler used in the electrophoresis gels. The concentrations used include 1000-fold, 100-fold, 10-fold dilutions and non-diluted samples. **Abbreviations**: NC (Negative Control); GR (GeneRuler); ND (Non diluted).

4.5.3 Deletion of TWR49273 in PrhoTΔpvdLΔtrbABC-44 abolished the ability to take up the *P. graminis* siderophore

To confirm that the identified receptor TWR49273 was indeed the receptor responsible for the uptake of the *P. graminis* siderophore, the receptor TWR49273 of the type strain of *P. rhodesiae* was deleted in the siderophore-negative mutant PrhoTΔpvdLΔtrbABC-44. Growth stimulation assays with purified *P. graminis* siderophore fractions were subsequently conducted with mutant PrhoTΔpvdLΔtrbABCΔTWR49273-159. The mutant lost the ability to take up *P. graminis* siderophore fractions (Figure 21), confirming that the predicted receptor TWR49273 of *P. rhodesiae* LMG 17764T is responsible for the uptake of the *P. graminis* siderophore.

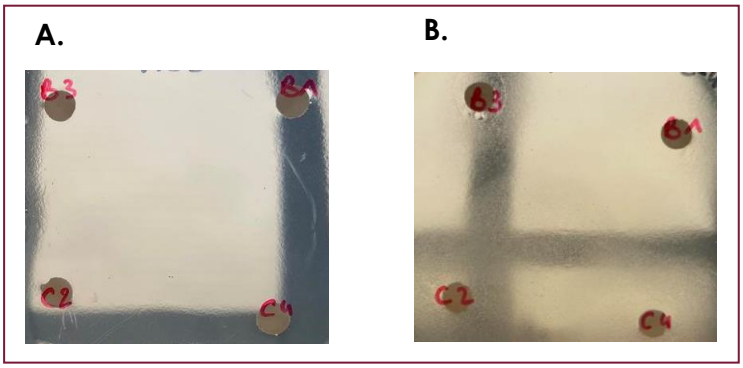

Figure 21: Growth stimulation assays of **A.** PrhoTΔpvdLΔtrbABCΔTWR49273-159 is not able to grow without the TWR49273-159 gene and **B**. PrhoTΔpvdLΔtrbABC-44 is able to grow with fractions of the *P. graminis* siderophore. **Abbreviations**: B3 = *m/z* 874.70, B1 = *m/z* 876.70, C2 = *m/z* 902.72 and C4 = *m/z* 904.72.

4.5. *P. lutea* group strains produce iron-regulated antimicrobial natural products which inhibit the growth of clinical strains

In vitro antagonism assays using *P. lutea* group strains (Table 3) revealed varying levels of growth inhibition of *S. capitis*, *C. albicans*, *S. enterica*, *P. aeruginosa*, *B. cereus* and *C. sporogenes*. For *E. coli* DV4951and *E. hirae* LMG 10274 no growth inhibition was observed (data not shown). The *P. graminis* strains showed similar zones of growth inhibition, but zones of the type strain were smaller than those of the other *P. graminis* strains (Figure 22). In contrast to the other strains, *P. graminis* P200/02 and P334/03 were not able to inhibit the growth of *C. albicans* (Figure 22).

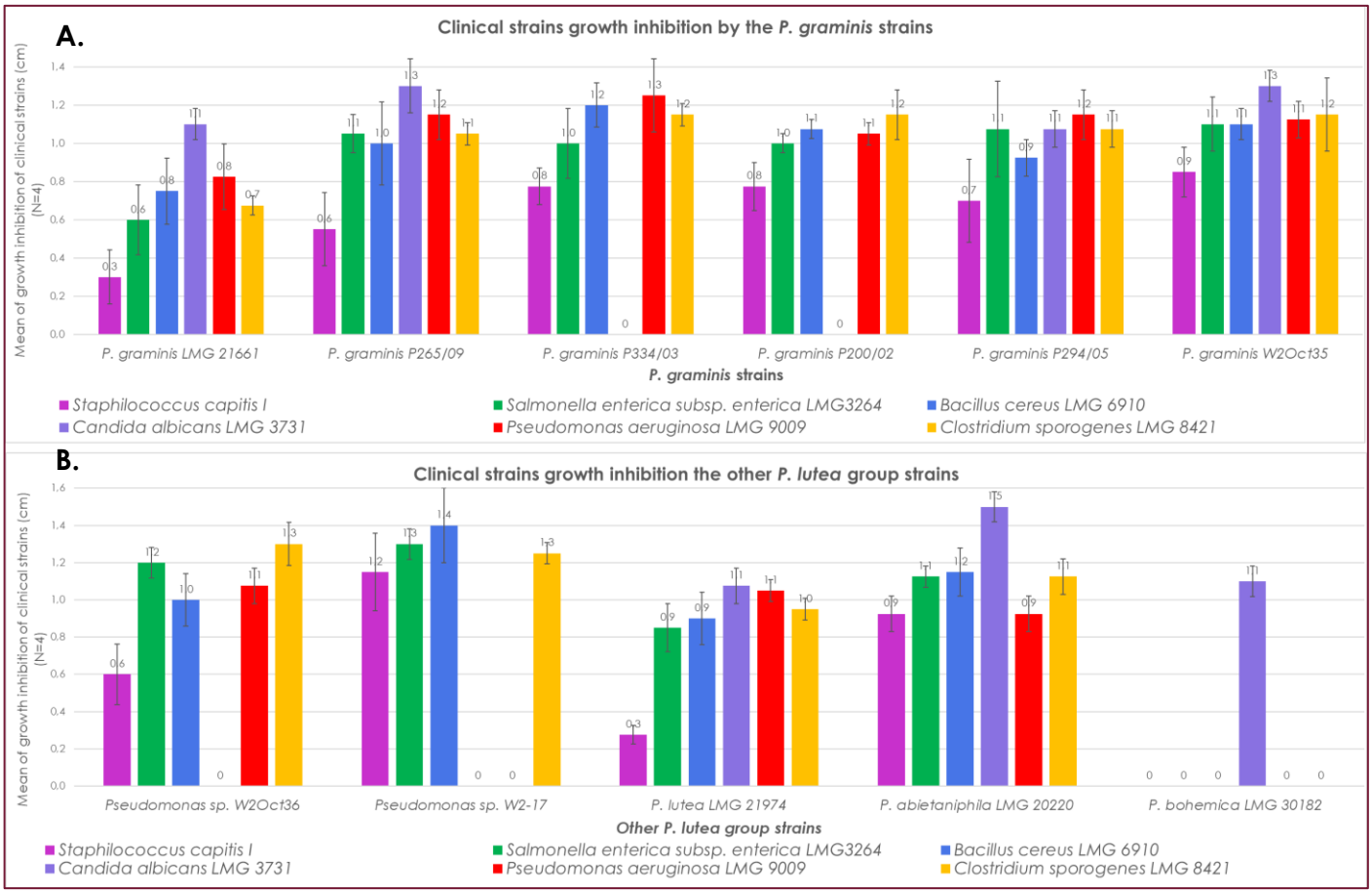

Figure 22: Growth inhibition area of clinical strains by **A.** *P. graminis* strains and **B.** other strains from the *P. lutea* group such as *P. lutea*, *P. abietaniphila* and *P. bohemica*. The area of growth inhibition has been measured from *P. lutea* group strain colony edge to the clinical strain debut of growth. Measures were taken on four replicates for each strain.

Strains W2Oct36 and W2-17 were able to inhibit the growth of most tested organisms, except for *C. albicans*. Strain W2-17 could also not inhibit *P. aeruginosa*. The type strains of *P. lutea* and *P. abietaniphila* were able to inhibit all the clinical strains. *P. bohemica* LMG 30182^T, which does not produce the *P. graminis* siderophore, had a hugely different profile, it was a weak antagonist, it only displayed growth inhibiting properties against *C. albicans* LMG 3731 (Figure 23).

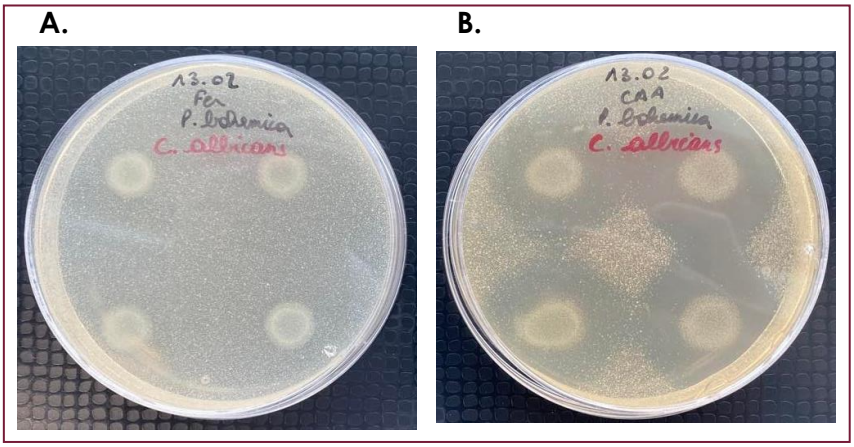

Figure 23: Inhibition of *Candida albicans* LMG 3731 growth by *P. bohemica* LMG 30182^T.
A. CAA medium with additional iron as a control where no growth inhibition is observed.
B. CAA medium without additional iron where growth inhibition is observed.

4.6 The *P. graminis* siderophore has *in vitro* antimicrobial properties against certain clinical strains

Results from antagonism assay with purified fractions of the *P. graminis* siderophore demonstrated growth inhibition of several clinical strains (Figure 24).

Four variants of the *P. graminis* siderophore on 6 (Table 8), represented by four different peaks (Peak A = *m/z* 874.70, Peak B = *m/z* 876.70, Peak C = *m/z* 902.72 and Peak D = *m/z* 904.72) purified by preparative HPLC have been investigated for their antimicrobial properties. These fractions showed growth inhibition properties on three of the studied clinical strains (Figure 24): *S. capitis* I, *B. cereus* LMG 6910 and *C. sporogenes* LMG 8421 (Figure 25).

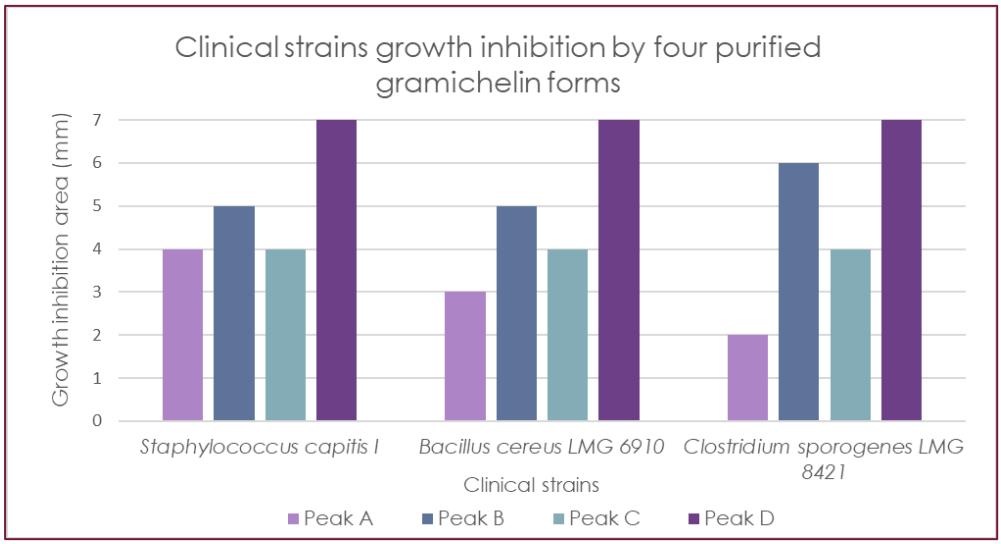

Figure 24: Growth inhibition area (mm) of *S. capitis* I, *B. cereus* LMG 6910, and *C. sporogenes* LMG 8421 by four variants of the *P. graminis* siderophore purified by preparative HPLC.

No growth inhibition was observed for *E. hirae* LMG 10274, *P. aeruginosa* LMG 9009, *E. coli* DV 495, *S. enterica subsp. enterica* LMG 3264 and *C. albicans* LMG 3731 as seen in Figure 25 for *C. albicans* LMG 3731.

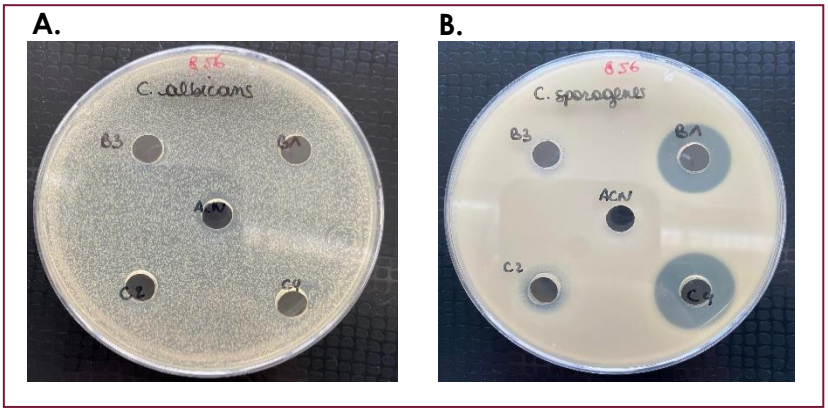

Figure 25: *In vitro* antagonism assays with variants of *P. graminis* siderophore. **A**. *Candida albicans* LMG 3731 growth is not inhibited by any variant. **B**. *Clostridium sporogenes* LMG 8421 growth is inhibited by the four studied variants of *P. graminis* siderophore. Acetonitrile 70% (ACN) is used as a control. **Abbreviations**: B3 = *m/z* 874.70, B1 = *m/z* 876.70, C2 = *m/z* 902.72 and C4 = *m/z* 904.72.

4.7 None of the strains of the *P. lutea* group can utilize pyoverdine

None of the *P. lutea* group strains was growth stimulated (Table 10) by any of the tested pyoverdines (Annex II) except for *P. bohemica* LMG 30182^T, which is weakly growth stimulated by a few structurally related pyoverdines that are probably taken up by the same receptor, probably not a pyoverdine receptor.

Table 10: Growth stimulation assay results of strains of the *P. lutea* group. Optimal concentrations of 2, 2'-bipyridine have been determined for each strain. A negative result is indicated by "-".

Strains	Optimal [2, 2'-bipyridine] (µM)	Results
***P. graminis* LMG 21661^T**	100-200	-
***P. graminis* P265/09**	100-200	-
***P. graminis* P334/03**	100-200	-
***P. graminis* P200/02**	100-200	-
***P. graminis* P294/05**	100-200	-
***P. graminis* W2Oct35**	100-200	-
***Pseudomonas sp.* W2Oct36**	100-200	-
***Pseudomonas sp.* W2-17**	100-200	-
***P. lutea* LMG 21974^T**	100-200	-
***P. abietaniphila* LMG 20220^T**	100-200	-
***P. bohemica* LMG 30182^T**	400-500	Weakly grow in presence of structural-related pyoverdines

5. Discussion

P. graminis is predicted to produce an amphiphilic siderophore

P. graminis sp. are environmental strains that have been isolated from diverse niches including plants and "watery" environments such as cloud water (Besaury et al., 2017) and river water (Matthijs et al., 2013). This work shows that the grass isolate *P. graminis* LMG 21661^T is predicted to produce marinobactins, a suite of amphiphilic siderophores, to cope with iron limitation. This result is based on *in silico* predictions of the siderophore gene cluster, and the purification of the siderophores followed by LC-MS analysis.

Marinobactins produced by *Marinobacter* sp. have a six amino acids long headgroup that coordinates iron(III) appended by a C12-C18 fatty acid (Martinez et al., 2000; Martinez and Butler, 2007). The rationale underlying the production of marinobactin by *Marinobacter* sp. might be to establish a gradient of varying hydrophobicities, positioning the more hydrophobic siderophores (those with longer lipopeptide tails) in proximity to the cell, while the more hydrophilic ones are located farther away from the cell. Amphiphilic siderophores represent nearly half of the known marine siderophores to avoid siderophore diffusion in oceanic environments (Martinez et al., 2003). It is predicted that the forms produced by *P. graminis* LMG 21661^T have shorter acyl chains (C8-C12). The shorter acyl chains could be an adaption to a more terrestrial lifestyle.

Further work showed that the *P. graminis* siderophore is in fact the typical siderophore produced by almost all the strains of the *P. lutea* group. The *P. lutea* group, belonging to the *P. fluorescens* lineage, consists out of five pyoverdine-negative species; *P. lutea*, *P. graminis*, *P. harudinis*, *P. abietaniphila*, and *P. bohemica*. *P. bohemica* LMG 30182^T is an exception in the *P. lutea* group. It does not have the *P. graminis* siderophore biosynthetic genes, only the receptor. The strain might once have been a *P. graminis* siderophore producer but lost its ability to produce the siderophore. This loss could indicate a cheating behavior, whereby the strain exploits the *P. graminis* siderophore produced by other organisms (Kramer et al., 2019).

In the genus *Pseudomonas,* not many amphiphilic siderophores are known. Certain plant-associated *Pseudomonas* sp. such as *P. corrugata* spp., *P. fluorescens* SBW25, *Pseudomonas* sp. AF76 and *P. thivervalensis* spp. produce a siderophore that belongs to the corrugatin-family of siderophores (including corrugatin, ornicorrugatin, and histicorrugatin) (Matthijs et al., 2016, 2008; Risse et al., 1998). But the corrugatin-family of siderophores are single siderophores with a short fatty acid chain length (C8) as opposed to the predicted suite of marinobactins that have longer fatty acid tails that differ in length and saturation. In contrast to the predicted *P. graminis* siderophore corrugatin, ornicorrugatin, and histicorrugatin demonstrate no antimicrobial properties (*pers. comm*., Matthijs S.).

Various species that belong to other genera than *Pseudomonas* produce different amphiphilic siderophores. Examples include ornibactins produced by *Burkholderia cepacia*, acinetoferrin produced by *Acinetobacter haemolyticus*, rhizobactin produced by *Sinorhizobium meliloti*, and carboxymycobactins produced by mycobacteria.

They typically contain hydroxamate and/or catecholate functional groups, which are involved in iron coordination. However, their specific structural details, including the number and arrangement of these functional groups as well as their side chains, may differ. For example, ornibactins have variable side chains, acinetoferrin has a fatty acyl group, rhizobactin has an acyl group, and carboxymycobactins have acyl or peptidyl side chains (Agnoli et al., 2006; Fadeev et al., 2005; Rodriguez et al., 2008). These differences reflect the diversity of siderophore structures and their adaptations to specific bacterial species and environments (Leventhal et al., 2019).

***P. graminis* siderophore piracy**

Pseudomonas species generally produce one to three siderophores. They also encode additional TonB-dependent receptors that may allow them to utilize xenosiderophores, siderophores that are produced by other bacteria, including *Pseudomonas* and fungi (Cornelis and Dingemans, 2013; Matthijs et al., 2009; Perraud et al., 2020).

To verify whether *Pseudomonas* strains not belonging to the *P. lutea* group possess a putative *P. graminis* siderophore receptor a BlastX analysis was done with *mrbG* and a high number of *Pseudomonas* strains with a putative *P. graminis* siderophore receptor was found. An analysis of these strains is out of the scope of this work. But for some of the candidates for which siderophore-negative mutants were present in the NaturaMonas *Pseudomonas* collection it was verified through growth stimulation assays whether they were growth-stimulated by the *P. graminis* siderophore.

The tested strains were the siderophore-negative mutants of strain *P. rhodesiae* LMG 17764^T, *P. simiae* WCS417, *P. capeferrum* WCS358, *Pseudomonas* sp. WCS374, *P. fluorescens* SBW25 and *P. azotoformans* LMG 21611^T. They were all growth stimulated by the semi-purified *P. graminis* siderophore and purified siderophore fractions. These results indicate that *P. graminis* siderophore utilization is probably not uncommon among *Pseudomonas* sp. These strains were probably never *P. graminis* siderophore producers themselves but acquired the receptors through horizontal gene transfer from other bacteria.

To confirm that the predicted *P. graminis* siderophore receptor in these strains was indeed responsible for the uptake of the *P. graminis* siderophore, the receptor with accession code TWR49273 was deleted in the siderophore-negative mutant Prho^{T}ΔpvdLΔtrbABC-44 of *P. rhodesiae* LMG 17764^T and the growth stimulation experiments were repeated. Based on the

obtained results, it was confirmed that the receptor TWR49273 is responsible for the uptake of the *P. graminis* siderophore. The TWR49273 receptor of *P. rhodesiae* shows high levels of identity at the amino acid level to the putative *P. graminis* siderophore receptor of *P. simiae* WCS417 (94.3%), *Pseudomonas* sp. WCS374 (91.6%) and *P. fluorescens* SBW25 (94.7%). These results corroborate that the predicted *P. graminis* siderophore receptor of these three strains is indeed the receptor for the *P. graminis* siderophore.

Pyoverdine-mediated iron uptake for strains of the *P. lutea* group

The predicted number of TonB-dependent receptors, based on the analysis of their translated genomes, is relatively low for the type strains of the *P. lutea* group. *P. lutea* LMG 21974^T, *P. abietaniphila* LMG 20220^T and *P. graminis* DSM 11363^T have respectively 9, 10, and 14 TonB-dependent receptors whereas *P. bohemica* LMG 30182^T has a significant higher number, namely 31. The presence of more TonB-dependent receptors could make *P. bohemica* a stronger competitor in nutrient-limiting conditions than the type strains of *P. lutea*, *P. abietaniphila,* and *P. graminis* since it probably is able to pirate more siderophores from other bacteria and fungi. The higher number of TonB-dependent receptors than its phylogenetic neighbours could therefore "compensate" for the loss of the predicted marinobactin biosynthesis genes.

Not much is yet known about the nature of the molecules transported by most TonB-dependent receptors. Nothing is known about the xenosiderophores that can be utilized by *P. graminis* and other strains of the *P. lutea* group. It was therefore verified whether *P. graminis* and the other strains of the *P. lutea* group in our collection, which are all pyoverdine-negative, were able to use pyoverdines by means of growth stimulation assays. Pyoverdines are very competent iron scavengers produced by most members of the *Pseudomonas* genus. Surprisingly, none of the strains was growth stimulated by pyoverdine despite that a large and representative collection of pyoverdines has been tested. A weak stimulation was observed for a few pyoverdines for *P. bohemica*, but this observation was probably due to a weak uptake by another receptor. These results seem to indicate that pyoverdine-mediated competition for iron is not important for these strains.

These results not only contribute to our knowledge of the *P. graminis* siderophore uptake but also offer valuable insights into the versatility and adaptability of bacterial strains when it comes to iron acquisition strategies. Understanding the uptake of the *P. graminis* siderophore in diverse strains expands the scope of research in this field and opens avenues for future investigations into the ecological and evolutionary aspects of siderophore utilization in bacteria.

***In vitro* antimicrobial properties of the *P. graminis* siderophore**

In vitro antagonism assays conducted using strains of the *P. lutea* group revealed their ability to inhibit the growth of several clinical pathogens under iron-limiting conditions. These strains

exhibited significant inhibitory effects on the growth of most tested clinical strains, except for *E. coli* DV 4951 and *E. hirae* LMG 10274.

Notably, the growth inhibition of *C. albicans* LMG 3731 by *P. lutea* LMG 21974^T, *P. abietaniphila* LMG 20220^T, and P. *graminis* species LMG 21661^T, P294/05, and W2Oct35 was likely attributed to the presence of an antifungal natural product that is produced under iron-limiting conditions. Conversely, *P. graminis* species P265/09 and P334/03, as well as *Pseudomonas* sp. W2Oct36, did not produce this antifungal natural product against *C. albicans* LMG 3731, as they were incapable of inhibiting its growth under the experimental conditions used.

In the case of *P. bohemica* LMG 30182^T, it displayed growth-inhibiting properties exclusively against *C. albicans* LMG 3731, suggesting the production of a potential antifungal molecule. Additionally, a previous study conducted in 2018 (Saati-Santamaría et al., 2018) reported the growth-inhibiting activity of *P. bohemica* LMG 30182^T against *Candida humilis*.

The observation that the *P. graminis* siderophore producing strains were able to inhibit *C. sporogenes* LMG 8424, *S. capitis* I, and *B. cereus* LMG 6910 and the strain that did not produce this siderophore (*P. bohemica* LMG 30182^T) did not, in combination with the observation that the antagonism was repressed by iron, indicates that the *P. graminis* siderophore could play a role. To investigate this, the siderophore was isolated and tested against the same set of clinical strains. Remarkably, purified fractions of the *P. graminis* siderophore inhibited the growth of the three clinical strains. Conversely, the growth inhibition observed in *S. enterica* subsp. *enterica* LMG 3264 and *P. aeruginosa* LMG 9009 was attributed to another bactericidal natural product whose production is repressed by iron, as the purified *P. graminis* siderophore did not exhibit growth-inhibiting properties against them.

These findings underscore the diverse antagonistic capabilities of the examined strains and the production of multiple natural products contributing to their inhibitory effects on different clinical strains. Further research should focus on elucidating the specific mechanisms of action underlying these natural products and exploring their potential applications in antimicrobial therapies.

Moreover, these findings also validate the potential of the *P. graminis* siderophore as a naturally occurring growth-inhibiting agent produced by most strains of the *P. lutea* group. The antagonistic properties of this siderophore imply its role in suppressing the growth of competing microorganisms, thereby granting a competitive advantage to the producing strains within their ecological niche. Furthermore, these findings may have implications for the development of novel antimicrobial strategies that harness the antimicrobial potential of the *P. graminis* siderophore. Further investigations should delve into unraveling the molecular mechanisms underlying its growth-inhibiting properties, as well as exploring its specific mode of action against diverse bacterial species.

Perspectives

Regrettably, the complete structural elucidation of the predicted marinobactin or *P. graminis* siderophore remains unresolved in our study. Therefore, it is crucial to undertake further investigations employing tandem mass spectrometry (MS/MS) analyses and, if necessary, nuclear magnetic resonance (NMR) techniques to gain a comprehensive understanding of the siderophore's structure, including fragmentation patterns of its different adducts. These advanced analytical approaches will enable a more in-depth characterization and provide crucial insights into the molecular composition and architecture of the siderophore.

In our employed siderophore purification method, which selectively isolates the most hydrophilic siderophores, it is possible that more hydrophobic variants were missed due to the relatively low concentration of acetonitrile (70%) used for elution of the siderophores in the initial purification step. Thus, it is recommended to test higher acetonitrile concentrations to capture a broader range of siderophores. Additionally, as highlighted by Galvis et al., 2020, it is important to purify both the culture supernatant and the cell pellet to identify all possible forms of amphiphilic siderophores, including both the cell-free and cell-associated forms. Therefore, further investigations dedicated to characterizing additional forms of the *P. graminis* siderophore are warranted.

An interesting observation is that a siderophore with a predicted peptide chain identical to marinobactin is produced by *P. mendocina* ymp (Awaya and Dubois, 2008). Since this strain is not present in the NaturaMonas *Pseudomonas* collection, the closely related *P. mendocina* LMG 1223^T strain was investigated. It produced probably a siderophore with identical masses but different retention times, each variant eluted 3 minutes earlier. The difference in retention times indicates a structural difference between the *P. graminis* siderophore and the *P. mendocina* siderophore. However, due to time constraints, and the preliminary nature of the LC-MS data, the results were omitted from the current work. Nonetheless, this siderophore merits further investigation, especially considering its potential antimicrobial properties and its divergence from strains of the *P. lutea* group. Indeed, the strain showed very strong *in vitro* growth inhibition against all the tested clinical strains, except *against P. aeruginosa*

In light of these considerations, several perspectives can be pursued. Firstly, it is crucial to further investigate the potential broad-spectrum antimicrobial activity of the *P. graminis* siderophore, including phytopathogens. This will not only provide insights into its effectiveness against different pathogens but also aid in understanding the mechanisms underlying its growth-inhibiting properties, specifically its interaction with iron. Additionally, studying the siderophore's affinity for other metals is of significant importance to determine if it has the ability to bind to alternative metal ions. These perspectives will contribute to a comprehensive understanding of the *P. graminis* siderophore, its antimicrobial potential, and its metal-binding properties.

6. Conclusion

In conclusion, this study focused on the prediction and characterization of an amphiphilic siderophore produced by *Pseudomonas graminis* LMG 21661^T. The findings revealed that *P. graminis*, an environmental strain isolated from various niches, is likely capable of producing new variants of marinobactins, a suite of amphiphilic siderophores, as an adaptive response to iron limitation. These predictions were based on *in silico* analyses of the siderophore gene cluster and subsequent purification and LC-MS analysis of the **siderophores**.

The study also explored the siderophore piracy in *Pseudomonas* strains not belonging to the *P. lutea* group, indicating the acquisition of the *P. graminis* siderophore receptor through horizontal gene transfer. Growth stimulation assays confirmed the ability of these strains to utilize *the P. graminis* siderophore, further supporting the prevalence of siderophore utilization among *Pseudomonas* species.

Additionally, the study examined the pyoverdine-mediated iron uptake and antimicrobial properties of the *P. graminis* siderophore. Interestingly, the tested strains of the *P. lutea* group, which are pyoverdine-negative, showed significant inhibitory effects on the growth of various clinical pathogens under iron-limiting conditions. The antimicrobial properties of the siderophore were validated through *in vitro* antagonism assays using purified siderophore.

Although the complete structural elucidation of the predicted marinobactin or *P. graminis* siderophore remains unresolved, further investigations using advanced analytical techniques such as tandem mass spectrometry (MS/MS) and nuclear magnetic resonance (NMR) are recommended. Additionally, optimizing the purification method and exploring higher acetonitrile concentrations may provide a more comprehensive understanding of the siderophore's composition and capture a broader range of siderophores.

Overall, this study expands our knowledge of siderophore utilization and highlights the versatility and adaptability of bacterial strains in iron acquisition strategies. The findings offer valuable insights into the ecological and evolutionary aspects of siderophore utilization and present potential applications in antimicrobial therapies against MDR bacteria. Further research should focus on unraveling the molecular mechanisms and mode of action of the *P. graminis* siderophore, as well as exploring its broader antimicrobial potential against diverse bacterial or fungal species.

7. Bibliography

Abusnina, W., Shehata, M., Karem, E., Koc, Z., Khalil, E., 2019. Clostridium sporogenes bacteremia in an immunocompetent patient. IDCases 15, e00481. https://doi.org/10.1016/j.idcr.2018.e00481

Agnoli, K., Lowe, C.A., Farmer, K.L., Husnain, S.I., Thomas, M.S., 2006. The ornibactin biosynthesis and transport genes of Burkholderia cenocepacia are regulated by an extracytoplasmic function sigma factor which is a part of the Fur regulon. J. Bacteriol. 188, 3631–3644. https://doi.org/10.1128/JB.188.10.3631-3644.2006

Al Shaer, D., Al Musaimi, O., de la Torre, B.G., Albericio, F., 2020. Hydroxamate siderophores: Natural occurrence, chemical synthesis, iron binding affinity and use as Trojan horses against pathogens. Eur. J. Med. Chem. 208, 112791. https://doi.org/10.1016/j.ejmech.2020.112791

Al-Kuraishy, H.M., Al-Gareeb, A.I., 2017. Comparison of deferasirox and deferoxamine effects on iron overload and immunological changes in patients with blood transfusion-dependent β-thalassemia. Asian J. Transfus. Sci. 11, 13–17. https://doi.org/10.4103/0973-6247.200768

Awaya, J.D., Dubois, J.L., 2008. Identification, isolation, and analysis of a gene cluster involved in iron acquisition by Pseudomonas mendocina ymp. Biometals Int. J. Role Met. Ions Biol. Biochem. Med. 21, 353–366. https://doi.org/10.1007/s10534-007-9124-5

Behrendt, U., Ulrich, A., Schumann, P., Erler, W., Burghardt, J., Seyfarth, W., 1999. A taxonomic study of bacteria isolated from grasses: a proposed new species Pseudomonas graminis sp. nov. Int. J. Syst. Bacteriol. 49 Pt 1, 297–308. https://doi.org/10.1099/00207713-49-1-297

Besaury, L., Amato, P., Wirgot, N., Sancelme, M., Delort, A.M., 2017. Draft Genome Sequence of Pseudomonas graminis PDD-13b-3, a Model Strain Isolated from Cloud Water. Genome Announc. 5, e00464-17. https://doi.org/10.1128/genomea.00464-17

Bottone, E.J., 2010. Bacillus cereus, a Volatile Human Pathogen. Clin. Microbiol. Rev. 23, 382–398. https://doi.org/10.1128/CMR.00073-09

Bourafa, N., Loucif, L., Boutefnouchet, N., Rolain, J.-M., 2015. Enterococcus hirae, an unusual pathogen in humans causing urinary tract infection in a patient with benign prostatic hyperplasia: first case report in Algeria. New Microbes New Infect. 8, 7–9. https://doi.org/10.1016/j.nmni.2015.08.003

Braun, V., Pramanik, A., Gwinner, T., Köberle, M., Bohn, E., 2009. Sideromycins: tools and antibiotics. Biometals 22, 3–13. https://doi.org/10.1007/s10534-008-9199-7

Butler, A., Harder, T., Ostrowski, A.D., Carrano, C.J., 2021. Photoactive siderophores: Structure, function and biology. J. Inorg. Biochem. 221, 111457. https://doi.org/10.1016/j.jinorgbio.2021.111457

Cameron, D.R., Jiang, J.-H., Hassan, K.A., Elbourne, L.D.H., Tuck, K.L., Paulsen, I.T., Peleg, A.Y., 2015. Insights on virulence from the complete genome of Staphylococcus capitis. Front. Microbiol. 6, 980. https://doi.org/10.3389/fmicb.2015.00980

Carroll, C.S., Moore, M.M., 2018. Ironing out siderophore biosynthesis: a review of non-ribosomal peptide synthetase (NRPS)-independent siderophore synthetases. Crit. Rev. Biochem. Mol. Biol. 53, 356–381. https://doi.org/10.1080/10409238.2018.1476449

Chan, D.C.K., Burrows, L.L., 2023. Pseudomonas aeruginosa FpvB Is a High-Affinity Transporter for Xenosiderophores Ferrichrome and Ferrioxamine B. mBio 14, e0314922. https://doi.org/10.1128/mbio.03149-22

Chuljerm, H., Maneekesorn, S., Somsak, V., Ma, Y., Srichairatanakool, S., Koonyosying, P., 2021. Anti-Malarial and Anti-Lipid Peroxidation Activities of Deferiprone-Resveratrol Hybrid in Plasmodium berghei-Infected Mice. Biology 10, 911. https://doi.org/10.3390/biology10090911

Codd, R., 2023. 2.02 - Siderophores and iron transport, in: Reedijk, J., Poeppelmeier, K.R. (Eds.), Comprehensive Inorganic Chemistry III (Third Edition). Elsevier, Oxford, pp. 3–29. https://doi.org/10.1016/B978-0-12-823144-9.00044-3

Cornelis, P., Dingemans, J., 2013. Pseudomonas aeruginosa adapts its iron uptake strategies in function of the type of infections. Front. Cell. Infect. Microbiol. 3, 75. https://doi.org/10.3389/fcimb.2013.00075

Correnti, C., Strong, R.K., 2012. Mammalian Siderophores, Siderophore-binding Lipocalins, and the Labile Iron Pool *. J. Biol. Chem. 287, 13524–13531. https://doi.org/10.1074/jbc.R111.311829
Day, J.P., Ackrill, P., 1993. The chemistry of desferrioxamine chelation for aluminum overload in renal dialysis patients. Ther. Drug Monit. 15, 598–601. https://doi.org/10.1097/00007691-199312000-00026
De Vleesschauwer, D., Djavaheri, M., Bakker, P.A.H.M., Höfte, M., 2008. Pseudomonas fluorescens WCS374r-induced systemic resistance in rice against Magnaporthe oryzae is based on pseudobactin-mediated priming for a salicylic acid-repressible multifaceted defense response. Plant Physiol. 148, 1996–2012. https://doi.org/10.1104/pp.108.127878
Djavaheri, M., Mercado-Blanco, J., Versluis, C., Meyer, J.-M., Van Loon, L.C., Bakker, P.A.H.M., 2012. Iron-regulated metabolites produced by Pseudomonas fluorescens WCS374r are not required for eliciting induced systemic resistance against Pseudomonas syringae pv. tomato in Arabidopsis. MicrobiologyOpen 1, 311–325. https://doi.org/10.1002/mbo3.32
Duijff, B.J., Meijer, J.W., Bakker, P.A.H.M., Schippers, B., 1993. Siderophore-mediated competition for iron and induced resistance in the suppression of fusarium wilt of carnation by fluorescent Pseudomonas spp. Neth. J. Plant Pathol. 99, 277–289. https://doi.org/10.1007/BF01974309
Eng, S.-K., Pusparajah, P., Ab Mutalib, N.-S., Ser, H.-L., Chan, K.-G., Lee, L.-H., 2015. Salmonella: A review on pathogenesis, epidemiology and antibiotic resistance. Front. Life Sci. 8, 284–293. https://doi.org/10.1080/21553769.2015.1051243
Essén, S.A., Johnsson, A., Bylund, D., Pedersen, K., Lundström, U.S., 2007. Siderophore Production by Pseudomonas stutzeri under Aerobic and Anaerobic Conditions. Appl. Environ. Microbiol. 73, 5857–5864. https://doi.org/10.1128/AEM.00072-07
Fadeev, E.A., Luo, M., Groves, J.T., 2005. Synthesis and structural modeling of the amphiphilic siderophore rhizobactin-1021 and its analogs. Bioorg. Med. Chem. Lett., Symposium-in-Print: G-Protein-Coupled Receptors in Drug Discovery 15, 3771–3774. https://doi.org/10.1016/j.bmcl.2005.05.114
Fujii, I., Watanabe, A., Sankawa, U., Ebizuka, Y., 2001. Identification of Claisen cyclase domain in fungal polyketide synthase WA, a naphthopyrone synthase of Aspergillus nidulans. Chem. Biol. 8, 189–197. https://doi.org/10.1016/S1074-5521(00)90068-1
Fukushima, T., Kawabata, H., Nakamura, T., Iwao, H., Nakajima, A., Miki, M., Sakai, T., Sawaki, T., Fujita, Y., Tanaka, M., Masaki, Y., Hirose, Y., Umehara, H., 2011. Iron Chelation Therapy with Deferasirox Induced Complete Remission in a Patient with Chemotherapy-resistant Acute Monocytic Leukemia. Anticancer Res. 31, 1741–1744.
Galvis, F., Ageitos, L., Martínez-Matamoros, D., Barja, J.L., Rodríguez, J., Lemos, M.L., Jiménez, C., Balado, M., 2020. The marine bivalve molluscs pathogen Vibrio neptunius produces the siderophore amphibactin, which is widespread in molluscs microbiota. Environ. Microbiol. 22, 5467–5482. https://doi.org/10.1111/1462-2920.15312
Golonka, R., Yeoh, B.S., Vijay-Kumar, M., 2019. The Iron Tug-of-War between Bacterial Siderophores and Innate Immunity. J. Innate Immun. 11, 249–262. https://doi.org/10.1159/000494627
Grosse, C., Brandt, N., Van Antwerpen, P., Wintjens, R., Matthijs, S., 2023. Two new siderophores produced by Pseudomonas sp. NCIMB 10586: The anti-oomycete non-ribosomal peptide synthetase-dependent mupirochelin and the NRPS-independent triabactin. Front. Microbiol. 14.
Hider, R.C., Kong, X., 2010. Chemistry and biology of siderophores. Nat. Prod. Rep. 27, 637–657. https://doi.org/10.1039/B906679A
Hoffmann, K.M., Goncuian, E.S., Karimi, K.L., Amendola, C.R., Mojab, Y., Wood, K.M., Prussia, G.A., Nix, J., Yamamoto, M., Lathan, K., Orion, I.W., 2020. Cofactor Complexes of DesD, a Model Enzyme in the Virulence-related NIS Synthetase Family. Biochemistry 59, 3427–3437. https://doi.org/10.1021/acs.biochem.9b00899
Ito, A., Kohira, N., Bouchillon, S.K., West, J., Rittenhouse, S., Sader, H.S., Rhomberg, P.R., Jones, R.N., Yoshizawa, H., Nakamura, R., Tsuji, M., Yamano, Y., 2016. In vitro antimicrobial activity of S-649266, a catechol-substituted siderophore cephalosporin, when tested against non-

fermenting Gram-negative bacteria. J. Antimicrob. Chemother. 71, 670–677. https://doi.org/10.1093/jac/dkv402
Kaper, J.B., Nataro, J.P., Mobley, H.L.T., 2004. Pathogenic Escherichia coli. Nat. Rev. Microbiol. 2, 123–140. https://doi.org/10.1038/nrmicro818
Khasheii, B., Mahmoodi, P., Mohammadzadeh, A., 2021. Siderophores: Importance in bacterial pathogenesis and applications in medicine and industry. Microbiol. Res. 250, 126790. https://doi.org/10.1016/j.micres.2021.126790
Konz, D., Marahiel, M.A., 1999. How do peptide synthetases generate structural diversity? Chem. Biol. 6, R39–R48. https://doi.org/10.1016/S1074-5521(99)80002-7
Kramer, J., Ozkaya, O., Kümmerli, R., 2019. Bacterial siderophores in community and host interactions. Nat. Rev. Microbiol. 18, 1–12. https://doi.org/10.1038/s41579-019-0284-4
Lamb, A.L., 2015. Breaking a pathogen's iron will: Inhibiting siderophore production as an antimicrobial strategy. Biochim. Biophys. Acta 1854, 1054–1070. https://doi.org/10.1016/j.bbapap.2015.05.001
Leventhal, G.E., Ackermann, M., Schiessl, K.T., 2019. Why microbes secrete molecules to modify their environment: the case of iron-chelating siderophores. J. R. Soc. Interface 16, 20180674. https://doi.org/10.1098/rsif.2018.0674
Lim, Y.P., Go, M.K., Yew, W.S., 2016. Exploiting the Biosynthetic Potential of Type III Polyketide Synthases. Molecules 21, 806. https://doi.org/10.3390/molecules21060806
Lun, S., Guo, H., Adamson, J., Cisar, J.S., Davis, T.D., Chavadi, S.S., Warren, J.D., Quadri, L.E.N., Tan, D.S., Bishai, W.R., 2013. Pharmacokinetic and in vivo efficacy studies of the mycobactin biosynthesis inhibitor salicyl-AMS in mice. Antimicrob. Agents Chemother. 57, 5138–5140. https://doi.org/10.1128/AAC.00918-13
Martinez, J.S., Butler, A., 2007. Marine amphiphilic siderophores: marinobactin structure, uptake, and microbial partitioning. J. Inorg. Biochem. 101, 1692–1698. https://doi.org/10.1016/j.jinorgbio.2007.07.007
Martinez, J.S., Carter-Franklin, J.N., Mann, E.L., Martin, J.D., Haygood, M.G., Butler, A., 2003. Structure and Membrane Affinity of a Suite of Amphiphilic Siderophores Produced by a Marine Bacterium. Proc. Natl. Acad. Sci. U. S. A. 100, 3754–3759. https://doi.org/10.1073/pnas.063744410
Martinez, J.S., Zhang, G.P., Holt, P.D., Jung, H.T., Carrano, C.J., Haygood, M.G., Butler, A., 2000. Self-assembling amphiphilic siderophores from marine bacteria. Science 287, 1245–1247. https://doi.org/10.1126/science.287.5456.1245
Marugg, J.D., van Spanje, M., Hoekstra, W.P., Schippers, B., Weisbeek, P.J., 1985. Isolation and analysis of genes involved in siderophore biosynthesis in plant-growth-stimulating Pseudomonas putida WCS358. J. Bacteriol. 164, 563–570. https://doi.org/10.1128/jb.164.2.563-570.1985
Matthijs, S., Brandt, N., Ongena, M., Achouak, W., Meyer, J.-M., Budzikiewicz, H., 2016. Pyoverdine and histicorrugatin-mediated iron acquisition in Pseudomonas thivervalensis. BioMetals 29, 467–485. https://doi.org/10.1007/s10534-016-9929-1
Matthijs, S., Budzikiewicz, H., Schäfer, M., Wathelet, B., Cornelis, P., 2008. Ornicorrugatin, a new siderophore from Pseudomonas fluorescens AF76. Z. Naturforschung C J. Biosci. 63, 8–12. https://doi.org/10.1515/znc-2008-1-202
Matthijs, S., Coorevits, A., Gebrekidan, T.T., Tricot, C., Wauven, C.V., Pirnay, J.-P., De Vos, P., Cornelis, P., 2013. Evaluation of oprI and oprL genes as molecular markers for the genus Pseudomonas and their use in studying the biodiversity of a small Belgian River. Res. Microbiol. 164, 254–261. https://doi.org/10.1016/j.resmic.2012.12.001
Matthijs, S., Laus, G., Meyer, J.-M., Abbaspour-Tehrani, K., Schäfer, M., Budzikiewicz, H., Cornelis, P., 2009. Siderophore-mediated iron acquisition in the entomopathogenic bacterium Pseudomonas entomophila L48 and its close relative Pseudomonas putida KT2440. Biometals Int. J. Role Met. Ions Biol. Biochem. Med. 22, 951–964. https://doi.org/10.1007/s10534-009-9247-y
Matthijs, S., Vander Wauven, C., Cornu, B., Ye, L., Cornelis, P., Thomas, C.M., Ongena, M., 2014. Antimicrobial properties of Pseudomonas strains producing the antibiotic mupirocin. Res. Microbiol. 165, 695–704. https://doi.org/10.1016/j.resmic.2014.09.009

Mayer, F.L., Wilson, D., Hube, B., 2013. Candida albicans pathogenicity mechanisms. Virulence 4, 119–128. https://doi.org/10.4161/viru.22913

Mikiciński, A., Sobiczewski, P., Puławska, J., Malusa, E., 2016. Antagonistic potential of Pseudomonas graminis 49M against Erwinia amylovora, the causal agent of fire blight. Arch. Microbiol. 198, 531–539. https://doi.org/10.1007/s00203-016-1207-7

Mootz, H.D., Schwarzer, D., Marahiel, M.A., 2002. Ways of Assembling Complex Natural Products on Modular Nonribosomal Peptide Synthetases. ChemBioChem 3, 490–504. https://doi.org/10.1002/1439-7633(20020603)3:6<490::AID-CBIC490>3.0.CO;2-N

Nivina, A., Yuet, K.P., Hsu, J., Khosla, C., 2019. Evolution and Diversity of Assembly-Line Polyketide Synthases. Chem. Rev. 119, 12524–12547. https://doi.org/10.1021/acs.chemrev.9b00525

Noinaj, N., Guillier, M., Barnard, T.J., Buchanan, S.K., 2010. TonB-dependent transporters: regulation, structure, and function. Annu. Rev. Microbiol. 64, 43–60. https://doi.org/10.1146/annurev.micro.112408.134247

Oves-Costales, D., Kadi, N., Fogg, M.J., Song, L., Wilson, K.S., Challis, G.L., 2007. Enzymatic Logic of Anthrax Stealth Siderophore Biosynthesis: AsbA Catalyzes ATP-Dependent Condensation of Citric Acid and Spermidine. J. Am. Chem. Soc. 129, 8416–8417. https://doi.org/10.1021/ja072391o

Paczosa, M.K., Mecsas, J., 2016. Klebsiella pneumoniae: Going on the Offense with a Strong Defense. Microbiol. Mol. Biol. Rev. MMBR 80, 629–661. https://doi.org/10.1128/MMBR.00078-15

Page, M.G.P., 2019. The Role of Iron and Siderophores in Infection, and the Development of Siderophore Antibiotics. Clin. Infect. Dis. 69, S529–S537. https://doi.org/10.1093/cid/ciz825

Pang, B., Chen, Y., Gan, F., Yan, C., Jin, L., Gin, J.W., Petzold, C.J., Keasling, J.D., 2020. Investigation of Indigoidine Synthetase Reveals a Conserved Active-Site Base Residue of Nonribosomal Peptide Synthetase Oxidases. J. Am. Chem. Soc. 142, 10931–10935. https://doi.org/10.1021/jacs.0c04328

Patil, G.S., Kinatukara, P., Mondal, S., Shambhavi, S., Patel, K.D., Pramanik, S., Dubey, N., Narasimhan, S., Madduri, M.K., Pal, B., Gokhale, R.S., Sankaranarayanan, R., 2021. A universal pocket in fatty acyl-AMP ligases ensures redirection of fatty acid pool away from coenzyme A-based activation. eLife 10, e70067. https://doi.org/10.7554/eLife.70067

Peix, A., Ramírez-Bahena, M.-H., Velázquez, E., 2018. The current status on the taxonomy of Pseudomonas revisited: An update. Infect. Genet. Evol. 57, 106–116. https://doi.org/10.1016/j.meegid.2017.10.026

Perraud, Q., Cantero, P., Roche, B., Gasser, V., Normant, V.P., Kuhn, L., Hammann, P., Mislin, G.L.A., Ehret-Sabatier, L., Schalk, I.J., 2020. Phenotypic Adaption of Pseudomonas aeruginosa by Hacking Siderophores Produced by Other Microorganisms. Mol. Cell. Proteomics MCP 19, 589–607. https://doi.org/10.1074/mcp.RA119.001829

Qin, S., Xiao, W., Zhou, C., Pu, Q., Deng, X., Lan, L., Liang, H., Song, X., Wu, M., 2022. Pseudomonas aeruginosa: pathogenesis, virulence factors, antibiotic resistance, interaction with host, technology advances and emerging therapeutics. Signal Transduct. Target. Ther. 7, 1–27. https://doi.org/10.1038/s41392-022-01056-1

Quadri, L.E.N., 2014. Biosynthesis of mycobacterial lipids by polyketide synthases and beyond. Crit. Rev. Biochem. Mol. Biol. 49, 179–211. https://doi.org/10.3109/10409238.2014.896859

Ratledge, C., Dover, L.G., 2000. Iron Metabolism in Pathogenic Bacteria. Annu. Rev. Microbiol. 54, 881–941. https://doi.org/10.1146/annurev.micro.54.1.881

Reimer, J.M., Eivaskhani, M., Harb, I., Guarné, A., Weigt, M., Schmeing, T.M., 2019. Structures of a dimodular nonribosomal peptide synthetase reveal conformational flexibility. Science 366, eaaw4388. https://doi.org/10.1126/science.aaw4388

Risse, D., Beiderbeck, H., Taraz, K., Budzikiewicz, H., Gustine, D., 1998. Corrugatin, a Lipopeptide Siderophore from Pseudomonas corrugata. Z. Für Naturforschung C 53, 295–304. https://doi.org/10.1515/znc-1998-5-601

Rodriguez, G.M., Gardner, R., Kaur, N., Phanstiel, O., 2008. Utilization of Fe3+-acinetoferrin analogs as an iron source by Mycobacterium tuberculosis. BioMetals 21, 93–103. https://doi.org/10.1007/s10534-007-9096-5

Saati-Santamaría, Z., López-Mondéjar, R., Jiménez-Gómez, A., Díez-Méndez, A., Větrovský, T., Igual, J.M., Velázquez, E., Kolarik, M., Rivas, R., García-Fraile, P., 2018. Discovery of Phloeophagus Beetles as a Source of Pseudomonas Strains That Produce Potentially New Bioactive Substances and Description of Pseudomonas bohemica sp. nov. Front. Microbiol. 9.

Sabatini, M., Comba, S., Altabe, S., Recio-Balsells, A.I., Labadie, G.R., Takano, E., Gramajo, H., Arabolaza, A., 2018. Biochemical characterization of the minimal domains of an iterative eukaryotic polyketide synthase. Febs J. 285, 4494–4511. https://doi.org/10.1111/febs.14675

Saha, P., Yeoh, B.S., Xiao, X., Golonka, R.M., Kumarasamy, S., Vijay-Kumar, M., 2019. Enterobactin, an iron chelating bacterial siderophore, arrests cancer cell proliferation. Biochem. Pharmacol. 168, 71–81. https://doi.org/10.1016/j.bcp.2019.06.017

Saha, R., Saha, N., Donofrio, R.S., Bestervelt, L.L., 2013. Microbial siderophores: a mini review. J. Basic Microbiol. 53, 303–317. https://doi.org/10.1002/jobm.201100552

Schnider-Keel, U., Seematter, A., Maurhofer, M., Blumer, C., Duffy, B., Gigot-Bonnefoy, C., Reimmann, C., Notz, R., Défago, G., Haas, D., Keel, C., 2000. Autoinduction of 2,4-diacetylphloroglucinol biosynthesis in the biocontrol agent Pseudomonas fluorescens CHA0 and repression by the bacterial metabolites salicylate and pyoluteorin. J. Bacteriol. 182, 1215–1225. https://doi.org/10.1128/JB.182.5.1215-1225.2000

Schwyn, B., Neilands, J.B., 1987. Universal chemical assay for the detection and determination of siderophores. Anal. Biochem. 160, 47–56. https://doi.org/10.1016/0003-2697(87)90612-9

Shanzer, A., Libman, J., Lytton, S.D., Glickstein, H., Cabantchik, Z.I., 1991. Reversed siderophores act as antimalarial agents. Proc. Natl. Acad. Sci. U. S. A. 88, 6585–6589.

Sia, A.K., Allred, B.E., Raymond, K.N., 2013. Siderocalins: Siderophore binding proteins evolved for primary pathogen host defense. Curr. Opin. Chem. Biol. 17, 150–157. https://doi.org/10.1016/j.cbpa.2012.11.014

Sieber, S.A., Marahiel, M.A., 2005. Molecular Mechanisms Underlying Nonribosomal Peptide Synthesis: Approaches to New Antibiotics. Chem. Rev. 105, 715–738. https://doi.org/10.1021/cr0301191

Tiwari, R., Checkley, L., Ferdig, M.T., Vennerstrom, J.L., Miller, M.J., 2023. Synthesis and antimalarial activity of amide and ester conjugates of siderophores and ozonides. Biometals Int. J. Role Met. Ions Biol. Biochem. Med. 36, 315–320. https://doi.org/10.1007/s10534-022-00375-8

Tripathi, A., Schofield, M.M., Chlipala, G.E., Schultz, P.J., Yim, I., Newmister, S.A., Nusca, T.D., Scaglione, J.B., Hanna, P.C., Tamayo-Castillo, G., Sherman, D.H., 2014. Baulamycins A and B, Broad-Spectrum Antibiotics Identified as Inhibitors of Siderophore Biosynthesis in Staphylococcus aureus and Bacillus anthracis. J. Am. Chem. Soc. 136, 1579–1586. https://doi.org/10.1021/ja4115924

Vindeirinho, J.M., Soares, H.M.V.M., Soares, E.V., 2021. Modulation of Siderophore Production by Pseudomonas fluorescens Through the Manipulation of the Culture Medium Composition. Appl. Biochem. Biotechnol. 193, 607–618. https://doi.org/10.1007/s12010-020-03349-z

Wilson, B.R., Bogdan, A.R., Miyazawa, M., Hashimoto, K., Tsuji, Y., 2016. Siderophores in Iron Metabolism: From Mechanism to Therapy Potential. Trends Mol. Med. 22, 1077–1090. https://doi.org/10.1016/j.molmed.2016.10.005

Yin, L., Shen, W., Liu, J.-S., Jia, A.-Q., 2022. 2-Hydroxymethyl-1-methyl-5-nitroimidazole, one siderophore inhibitor, occludes quorum sensing in Pseudomonas aeruginosa. Front. Cell. Infect. Microbiol. 12, 955952. https://doi.org/10.3389/fcimb.2022.955952